TESIS DOCTORAL

COMPENDIO DE PUBLICACIONES

DESIGN OF SELF-LOCKING PLANETARY GEAR TRAINS FOR REHABILITATION ENGINEERING AND MOBILITY DEVICES

DOCTORADO EN INGENIERÍA MECÁNICA Y DE ORGANIZACIÓN INDUSTRIAL

Presenta:
Gaspar Rodríguez Jiménez

Directores:
Francisco Javier Alonso Sánchez
David Rodríguez Salgado

Tutor:

José María del Castillo Granados

Sevilla, Diciembre de 2018

TESIS DOCTORAL

COMPENDIO DE PUBLICACIONES

DISEÑO DE TRENES DE ENGRANAJES PLANETARIOS AUTORRETENIBLES PARA INGENIERÍA DE REHABILITACIÓN Y DISPOSITIVOS DE MOBILIDAD

DOCTORADO EN INGENIERÍA MECÁNICA Y DE ORGANIZACIÓN INDUSTRIAL

Presenta:
Gaspar Rodríguez Jiménez

Directores:
Francisco Javier Alonso Sánchez
David Rodríguez Salgado

Tutor:

José María del Castillo Granados

Sevilla, Diciembre de 2018

"When you want to know how things really work, study them when they are coming apart"

William Gibson.

Resumen

El número de personas que padecen debilidad muscular y que necesitan dispositivos externos que asistan o rehabiliten su marcha es cada vez mayor. Existe una gran variedad de dispositivos que estos pacientes pueden utilizar, entre ellos las ortesis de rodilla con bloqueo durante la fase de apoyo. Este tipo de ortesis permiten un control de la articulación durante el ciclo de la marcha, tanto en la fase de balanceo, como en la fase de apoyo. Dentro de este grupo, la gran mayoría utilizan sensores y/o actuadores para su correcto funcionamiento.

En este contexto, esta tesis doctoral presenta un estudio y un desarrollo de una órtesis de rodilla con control en la fase de apoyo. El dispositivo es totalmente mecánico y se bloquea para cualquier ángulo de flexión de la rodilla. El sistema principal de este dispositivo es un tren de engranajes planetarios autorretenibles que se encarga, por un lado, de permitir el movimiento de la articulación durante la fase de balanceo de la marcha, y por otro, de bloquearlo durante la fase de apoyo ante la presencia de cualquier ángulo de flexión de la rodilla. De esta manera se consigue un control de la marcha sin necesidad de actuadores ni sensores.

A pesar de la gran evolución tecnológica de las sillas de ruedas, la mayoría de ellas siguen siendo de propulsión manual debido a bajo precio, ligereza, transportabilidad y capacidad de plegado. Sin embargo, uno de los grandes obstáculos para los usuarios de sillas de ruedas es la subida de rampas ya que suponen una barrera para el desarrollo de las actividades diarias. Además, la subida de pendientes requiere esfuerzos musculares elevados.

En este trabajo, se propone la adaptación de un sistema de engranajes planetarios a las sillas de ruedas manuales para facilitar la labor de subida de rampas a la vez que disminuir el esfuerzo ejercido por el usuario. Este mecanismo consiste en un sistema de engranajes planetarios autorretenible que permite la subida de rampa cuando el usuario empuja la silla, y bloquea el movimiento de la silla cuando no existe potencia de entrada. Al tener una relación de transmisión reductora, la subida de rampas se realiza con menor esfuerzo muscular y además no es necesario activar mecanismos externos de freno o bloqueo de las ruedas.

Los resultados han permitido desarrollar dos aplicaciones novedosas de los trenes de engranajes planetarios autorretenibles en el campo de la Biomecánica y más específicamente en los dispositivos de rehabilitación y asistencia. Por un lado, la nueva ortesis de rodilla permite ampliar los dispositivos de rehabilitación y ayuda a la mejora de la marcha mediante un sistema completamente mecánico, adaptable a cualquier usuario. Por otro, el mecanismo de propulsión para sillas de ruedas manuales mejora movilidad de los usuarios de sillas de ruedas manuales utilizando un mecanismo adaptable a cualquier usuario y a cualquier silla de rueda manual.

Abstract

Muscular weakness produced by different pathologies increases year after year. Numerous devices can be used by subjects to assist or rehabilitate gait, such as Stance-Control-Knee-Ankle-Foot-Orthoses (SCKAFOs). These devices permit control of the whole gait cycle, both during the swing phase and the stance phase of gait. The majority of these SCKAFOs use sensors or actuators for their functioning.

This thesis presents the development of a new SCKAFO which can be used on any subject. The device is fully mechanical and can self-lock under any knee flexion angle. The main component of the system is a Planetary Gear train (PGT) with self-locking capability. This permits the movement of the orthosis during the swing phase, and the locking of the device during the stance phase of gait. Consequently, subjects control the gait cycle without using any sensor or actuator.

Although wheelchairs have seen great technological improvements, the majority continue to be manually propelled because of their low prize, lightness, transportability and folding capacity. Ramp climbing requires great muscular effort and can be a major problem for wheelchair users, it often prevents such users from ascending ramps and can cause problems in their daily life.

The use of a planetary gear train as a mechanical propulsion system to facilitate the ramp climbing and consequently reduce muscular effort is shown. This system consists of a planetary gear train with self-locking capability and thus permits the user to climb ramps when propelling the wheelchair and to self-lock when there is no power input. The system is a speed reducer, which means that when the user ascends ramps significantly less muscular effort is required. In addition to this, when using a self-locking PGT no external actuation is required to brake the wheelchair.

In this work, two new applications of self-locking planetary gear trains in rehabilitation and assistive devices fields are presented. The first application, a new SCKAFO which assists gait in subjects with lower limb injuries, it uses a completely mechanical device suitable for any user. The second application, a propulsion system for manual wheelchairs, improves the mobility of manual wheelchair users using a system that can be adapted to any user and any manual wheelchair.

Agradecimientos

Me gustaría expresar mi gratitud a todas las personas que han compartido estos últimos cuatro años y que han hecho que todo esto sea posible:

A mis directores, Javier y David, por todo el apoyo recibido tanto personal como académico. Por la paciencia que han tenido, por los consejos recibidos y por la confianza que han tenido en mí, sin ellos no hubiera sido posible la realización de esta tesis. A mi tutor José María, por su orientación.

A mis compañeros de fatiga, Jorge, Paco, José Manuel y Javier, por las horas que hemos pasado juntos en el laboratorio. Por los viajes realizados, los momentos de risas, los cafés, gracias a vosotros se ha hecho más llevadero.

A los miembros del laboratorio de Biomecánica de la Universidad Liverpool John Moores y en especial al profesor Mark Robinson, por su dedicación durante los meses de mi estancia y por su apoyo durante estos últimos años.

A mis amigos, por escucharme siempre, por los buenos momentos pasados y los que quedan. A Fran, seguro que estás orgulloso de mí.

A la familia Catterall, por todo el apoyo recibido, por hacerme sentir como en mi casa.

A mis padres, mi hermana y mis tíos, no sólo por el apoyo durante estos cuatro años, sino por el cariño recibido desde siempre. A Liz, por todo el apoyo recibido durante tanto tiempo, por tu cariño en los momentos más duros, tu paciencia y comprensión, gracias a ti he conseguido hacerlo.

Muchas gracias a todos.

Acknowledgements

I would like to express my gratitude to those who have guided and assisted me over the last four years:

To my PhD advisors, Javier and David, for imparting me with so much knowledge and for their academic and personal support. For their patience, advice and confidence in me. Without my directors this thesis would not have been possible. To my tutor José María, for his guidance.

To my colleagues, Jorge, Paco, José Manuel and Javier, for all the hours spent together in the laboratory. For all the trips and congresses, the coffees and chats, thanks to you the hard times were more manageable.

To the Biomechanical team at Liverpool John Moores University and especially to professor Mark Robinson, for his dedication during my stay and his support over the last years.

To my friends, for so many good times and for the ones to come, and above all, for the laughter during the difficult days. To Fran, I am sure you are proud of me.

To the Catterall family, for all their support and interest, for always making me feel at home.

To my parents, my sister, my aunt and uncle, not only for their unconditional support through everything, but for their guidance, understanding and love. To Liz, for all your support and care through the good times and the bad times, your patience and understanding, thanks to you I have made it.

Thank you very much to all of you.

Index

Appendix

A complete copy of each publication on which this thesis is based is attached.

Introduction

The understanding of human motion Biomechanics is fundamental in the prevention and treatment of injuries. Biomechanical studies give information about mechanical properties of tissues as well as mechanical loads during motion. The data obtained is used by engineers to design assistive devices which are able to prevent injuries and improve daily activities in users with special needs. Thus, understanding the functional mobility of a patient is crucial to determine the need for an assistive device. There exists a range of mobility assistive devices which patients can use, namely crutches, canes, walkers, orthoses, and manual and electric wheelchairs.

In this thesis two new planetary gear trains applications for rehabilitation engineering and mobility devices are presented. The first application is a fully mechanical knee orthosis which locks itself when required, providing users with lower limb injuries biomechanical assistance and therefore improving their gait. The second application is a propulsion system for a manual wheelchair with a self-locking capability which improves the mobility of manual wheelchairs users.

Knee orthoses are devices that are used to improve or assist gait in users with pathologies that produce muscular weaknesses in lower limbs. These users cannot lock the knee while walking, therefore the forces produced must be absorbed by an external device to permit gait. In this thesis, the device that has been designed is included within the group of the Stance-Control-Knee-Ankle-Foot-Orthoses (SCKAFOs), which control the knee during the stance phase of the gait, locking the knee and allowing the flexion of the knee during the swing phase. The entire process can be accomplished through a completely mechanical system where the main component is a Planetary Gear Train (PGT) with self-locking property. The device is attached to the lower limb through a mechanism which consists of rods and is responsible for introducing power to the mechanical system.

Manual wheelchairs users find slopes a great problem for their daily mobility. Although in recent years laws have been established to facilitate wheelchair accessibility in buildings, long distance slopes continue to be an issue, especially those located in cities. Facing such ramps with a manual wheelchair is a challenge when considering factors such as physical condition and fatigue which both affect greatly the climbing, and descending to a minor extent. In this work a fully mechanical propulsion system suitable for any manual wheelchair is presented. This system facilitates climbing and descending long distanced slopes and it is also able to lock itself when the user ceases the power input.

The purpose of the research is to improve and expand the existing SCKAFOs and propulsion systems in manual wheelchairs by increasing their usability and portability, using only mechanical components instead of electrical or electronic actuators which depend on other devices, such as sensors. The development and results of this thesis have been presented in two journal papers and represent the main content of this thesis.

State of the Art

There are many devices that use locking systems for their performance. Usually, a locking system allows or prevents the relative motion between two different parts. Although no ideal locking device exists, every device should have some common features such as; multiple locking positions, high locking force and instantaneous switching between locking and motion position among others.

In the literature, a general classification of locking systems has not been found. An excellent approximation can be seen in Table 1 where locking devices are classified depending on their locking principle and their application in robotics [1]. This classification gathers most of the different locking primary systems which could potentially be applied to biomechanical devices. In this context, SCKAFOs permit a wider variety of locking systems than manual wheelchairs.

Table 1.
Classification of locking mechanisms by its locking principle and its activation.

		Locking Principle		
		Mechanical	**Friction**	**Singularity**
Activation	**Active**	Latches Ratchets Dog Clutches Hydraulic Locks	Electromagnetic Overrunning Self-Amplifying Capstans Piezoelectric Bi-stable Statically balanced Thermic	Four-bar linkages
	Passive	Latches Ratchets Cam based	Overrunning Non-backdrivable	Non-linear Transfer ratio

Active devices are those that need actuators to switch between locking positions, while passive devices do not require any of these electrical or electronical actuators. This work focuses on passive locking systems and in particular on non-backdrivable gears. A mechanism has the property of non-backdrivability if the motion can be transmitted in one direction, but not in the opposite.

The existing mechanisms which have this property are lead-screws and worm drives [1,2], which are displayed in Fig. 1. These non-backdrivables mechanisms have been used on multiple occasions, above all in robotics, like the Southampton hand [3], CyberHand [4], RTR II [5] andTBM [6]. Worm gears have been particularly used in an active knee orthosis [7] and in a hip orthosis [8]. In these types of mechanisms, shear friction between gears acts as the brake force. The non-backdrivability of the mechanism is assured with a mechanical efficiency of less than 0.5 [2].

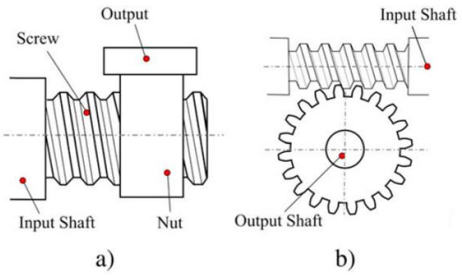

Fig. 1. a) Lead screw pair. b) Worm gear.

Non-backdrivability can also be achieved by using high reduction ratio transmission [9] due to the principle of virtual work and by using a customized clutch [9], where friction between fixed and driving parts is maximized. This work focuses on the condition of non-backdrivability in planetary gear trains.

Self-locking Planetary Gear Trains

Some Planetary Gear Trains (PGTs) with certain solutions and values of tooth ratios present the non-backdrivability property and act like a self-locking system. This property is mainly due to the friction between the elements and to geometrical reasons. When an external torque is applied to the output of a self-locking PGT, internal forces appear preventing the mechanism from moving. This particular condition is used in this thesis for the design of a new SCKAFO and a new propulsion system for a manual wheelchair with self-locking capability on ramps.

The first self-locking planetary gear train system was developed by Wolfrom [10]. It was formed by a sun gear, two planetary gears joined together through a planet carrier and two rings as shown in Fig. 2. The first analysis for this type of mechanism were developed by Looman [11] and Muller [12], which demonstrated that the system behaved differently depending on the operation mode. Thus, if the mechanism acts as a speed reducer, high transmission ratios can be achieved. However, if the system behaves as a speed multiplier, the self-locking condition appears [12].

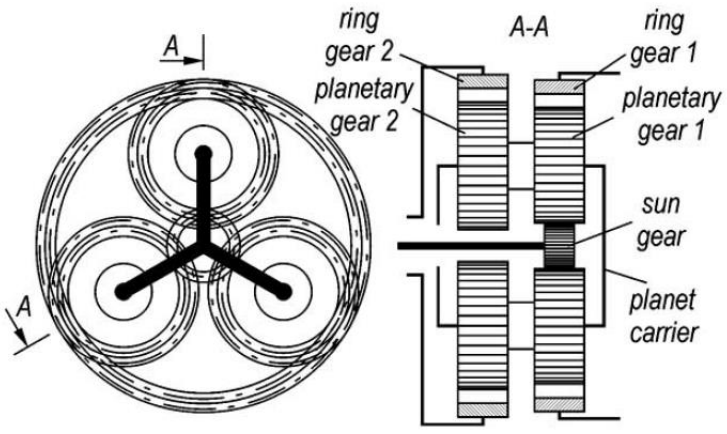

Fig. 2. Design of the Wolfrom PGT.

This particular condition of a Wolfrom PGT was used by Mihailidis [13] to generate high torques and test gearboxes in test rigs. Fig. 3 shows the test rig in which the Wolfrom

PGT is applied. It is evident that with small motors, high torques can be generated and the efficiencies of gearboxes can be calculated using these transmissions. When the main motor attemps to drive the output of the Wolfrom PGT, the self-locking condition appears and the PGT is locked without the usage of brakes. At this point, the stepper motor needs to drive the system and vary the torque or the system will rotate as a block.

Cesaroni [14] used a Wolfrom PGT at the output of the final wheel drive of electric trucks. Butsch [15], Orlowski [16] and Sulz [17] improved the Wolfrom PGT but no applications were carried out.

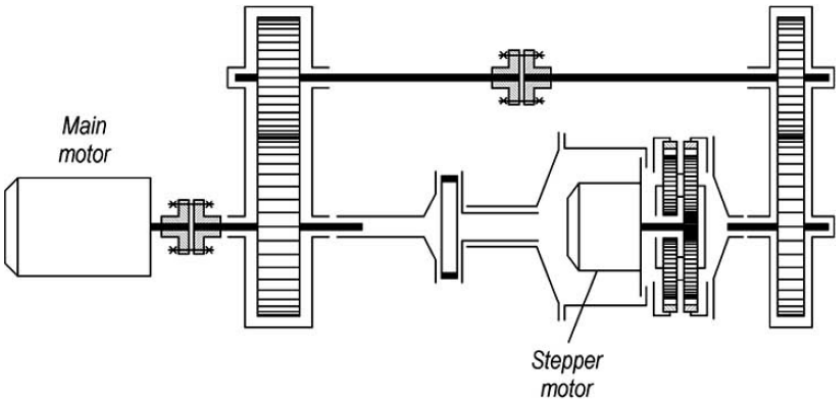

Fig. 3. Test rig using a Wolfrom PGT.

Other studies have been undertaken in order to determine the conditions for self-locking to appear [18] and also the efficiency of these transmissions [19-21]. Based on the literature, no application of self-locking planetary gear trains in the Biomechanics field was found.

On the contrary to other non-backdrivable mechanisms, self-locking PGTs are transmissions where the input and the output of the system are coaxial. This characteristic, together with the self-locking capability without any external brake or actuator, have allowed the use of self-locking PGTs to develop two fully mechanical devices with Biomechanical applications; a new SCKAFO and a new propulsion system for manual wheelchairs.

Stance-Control-Knee-Ankle-Foot-Orthosis

There are many SCKAFOS that use locking mechanisms to function, however, not many are completely mechanical. Having electrical or electronic components add more complexity to the control of the orthosis.

One of the first fully mechanical SCKAFOs was the Ottobock Bock Free Walk System [22] created by Becker Orthopædic UTX and presented in 1989 by Becker Orthopedic company. This system allows free flexion of the knee during the swing phase, and completely locks the knee during the stance phase. The main disadvantage of this orthosis is that the locking position is produced at full extension. Another disadvantage is that to switch between the stance phase and the swing phase, the user needs to produce a 10 degree dorsiflexion angle. The orthosis is presented in Fig. 4.

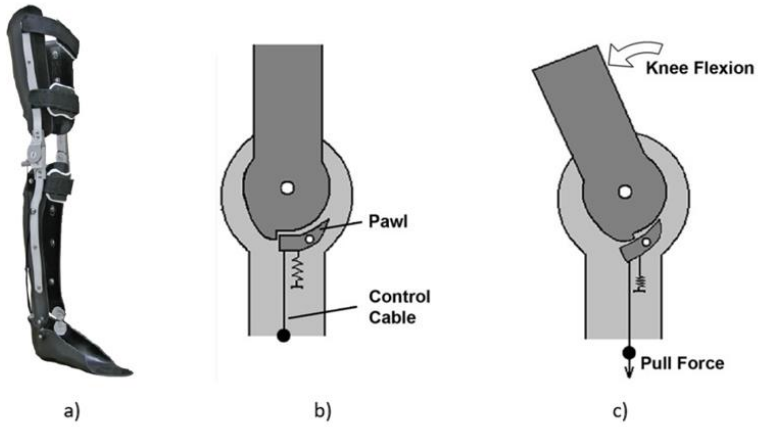

Fig. 4. a) Assembly of the Ottobock Bock Free Walk System. b) Locked position. c) Unlocked position

Another fully mechanical SCKAFO was developed by Fillauer and called Fillauer Swing Phase Lock [22]. In this case, the locking and unlocking of the mechanism was activated by gravity using a weighted pawl. The system improved the previous activation method, however it only permitted a locking position between 0 and 10 degrees of knee flexion. The functioning of this orthosis is displayed in Fig. 5. With this SCKAFO, the knee is locked during the stance phase and moves freely during the swing phase.

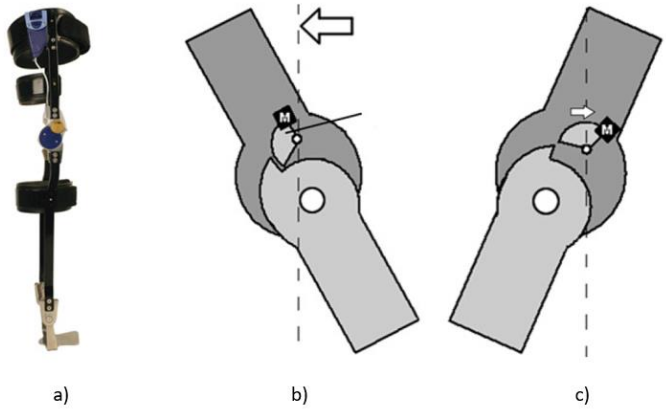

Fig. 5. a) View of the Fillauer Swing Phase Lock. b) Locked position. c) Unlocked position.

The Horton Stance Control Orthosis [22] used another type of mechanism to control the locking of the knee. During heel strike, a pushrod pushes a cam and locks the orthosis due to the contact against a friction ring. Once the contact with the ground disappears, the user is able to flex the knee. The orthosis allows the locking of the knee at any flexion angle, however, an extension moment is required to switch between the locking position and the unlocking position. This device is displayed in Fig. 6.

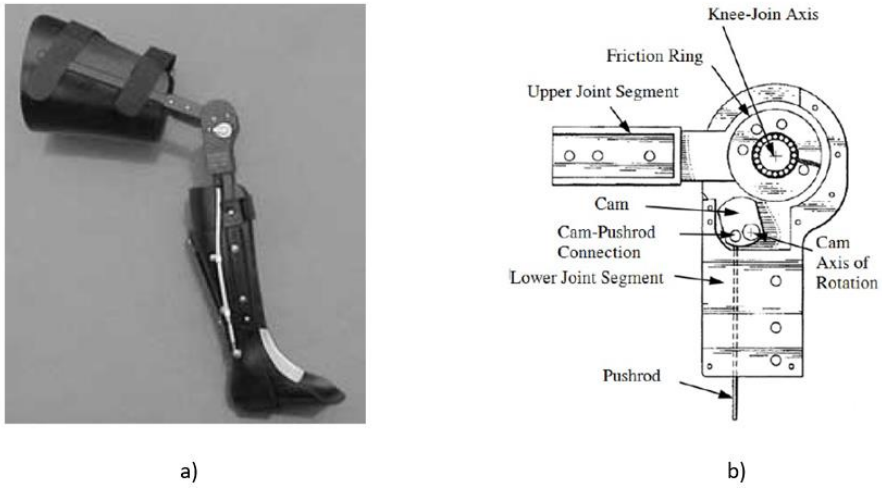

Fig. 6. a) View of the Horton Stance Control Orthosis. b) Locking mechanism.

A further fully mechanical SCKAFO was developed by Yakimovich et al. [22] which is able to both lock the knee at any flexion angle and permit the free rotation of the knee during the swing phase. The functioning of this orthosis is based on a belt that causes friction and thus increases the flexion resistance. Consequently, the joint locks. This orthosis is shown in Fig. 7 and although it controls the whole cycle of gait using a fully mechanical system, it requires a torsional torque to switch between the locking position and the unlocking position.

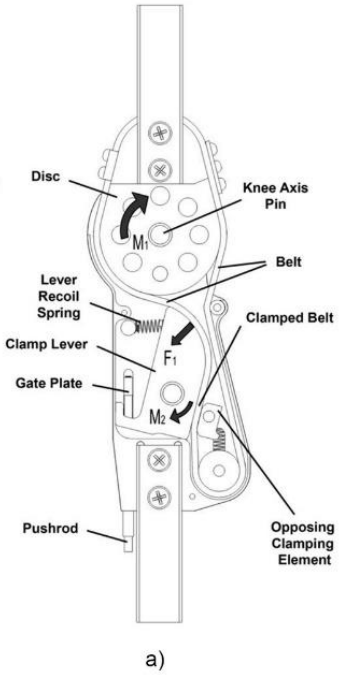

Fig. 7. a) Belt-clamping SCKAFO.

In [23] another SCKAFO is shown which allows the locking of the knee during the stance phase and allows the motion of the joint during the swing phase. The locking of the knee is achieved through a ratchet gear. This orthosis also allows the control of the flexion

during the stance phase of up to 15 degrees. However, its functioning is limited to the adjustment of a mechanical timer before its usage which allows the switch between swing and stance phase. This mechanical timer obliges the user to follow a selected speed which must be maintained throughout the gait cycle.

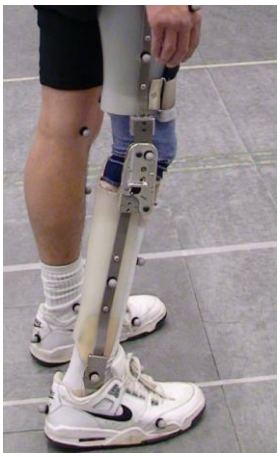

Fig. 8. View of the SCKAFO [23].

A new SCKAFO which permits the control of knee during the stance phase and allows to move the knee during the swing phase is presented. The SCKAFO proposed in this work has the following characteristics:

- The system is fully mechanical, it does not require any electronical or electrical actuators or sensors for its functioning.
- The control of the orthosis depends exclusively on the movement of the user.
- The system self-locks at any knee flexion angle.
- A torque to switch between the locking and the unlocking position is not required.
- The SCKAFO allows free motion during the swing phase.

Propulsion system for manual wheelchairs with self-locking capability.

Most of the manual wheelchairs (about 90%) that exist on the market are pushrim propelled [24]. However, there are other propulsion methods that can help users to reduce the physiological impact that pushrim propelled wheelchairs produce. The following are the most common [24]:

- Crank propelled wheelchair: Uses a bicycle propulsion system to facilitate the propulsion of the wheelchair (Fig. 9 a)).

- Lever propelled wheelchair: It is designed with manually operated push levers that transfer force to the wheels through a transmission mechanism (Fig. 9 b)).

- Hubcrank propelled wheelchair: The least common of the propulsion system, allows the user a continuous propulsion (Fig. 9 c)).

Fig. 9. a) Crank propelled. b) Lever propelled. c) Hubcrank propelled.

Each of these systems permits the adaptation of gear systems which facilitate the propulsion of manual wheelchairs during the climbing of steep ramps.

A further issue to consider in manual wheelchairs users is the braking of the wheelchair. People with low mobility can find this very important above all when they are situated on ramps. The most common system to reduce the speed applies friction to the wheels. On many occasions and depending on the gravity of the injury, this task can be very difficult. Some of the most used braking systems are as follows:

- Shoe brakes: Their use is the most extensive and they are designed in a way that can be activated by pushing forward or pulling backwards (Fig. 10 a)).
- Scissor brakes: They are mostly used by active subjects in sporty environments (Fig. 10 c)).
- One-hand brakes: This option is used by patients with hemiplegia (Fig. 10 b)).
- Drum brakes: They are mainly used when the wheelchair is pushed by another person as they are normally located on the backrest (Fig. 10 d)).

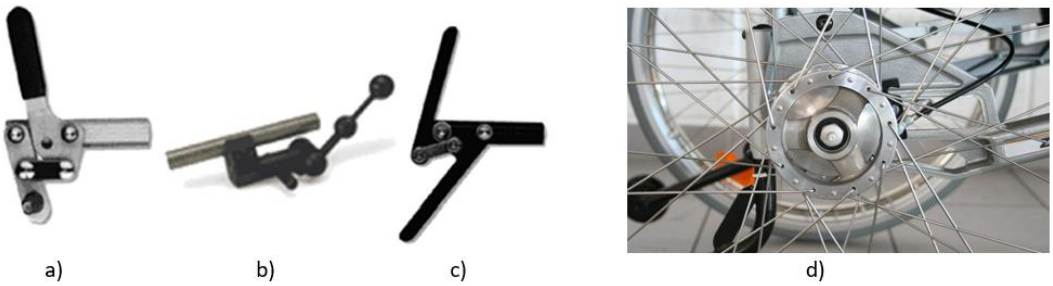

Fig. 10. a) Shoe brake. b) One-hand brake. a) Scissor brake. b) Drum brake.

All of these mechanisms require a manual activation and deactivation, which means that users must move or remove their hands in order to work the braking systems. However not all the mechanisms are manually activated, the system proposed in [25] is formed by a mechanical and automatic wheelchair brake which activates the brakes itself when a patient attempts to rise from the wheelchair (Fig. 11). The system consists of a three-way lever brake with three positions (locked, unlocked and automatic). There are other systems that automatically brake the wheels like those shown in [26, 27]

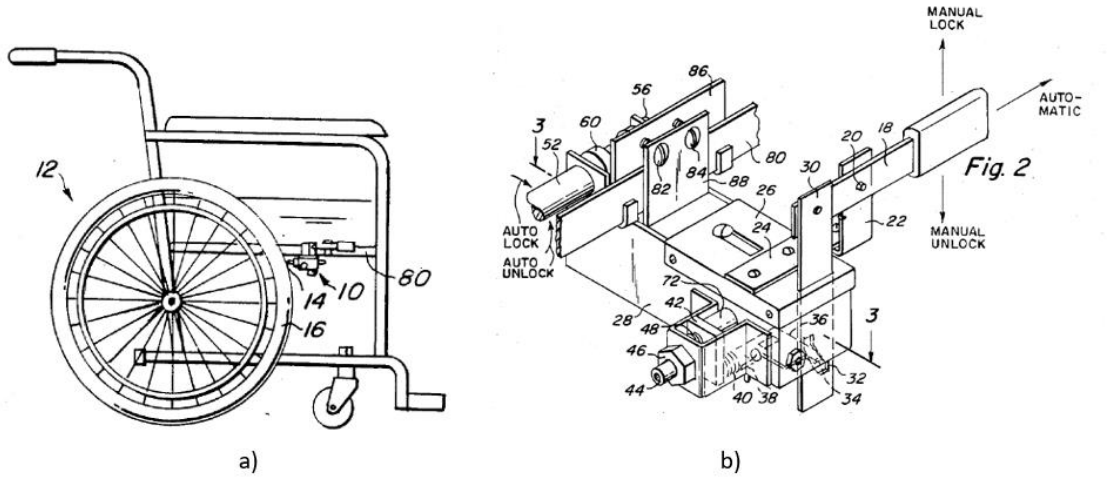

Fig. 11. a) Side view of the wheelchair. b) Three-mechanism.

As can be seen, there are many systems that are used to propel and brake a manual wheelchair. However, not many systems allow the user to both push the wheelchair and brake the system when required.

A system proposed by [28] whose commercial name is MagicWheel (Fig. 12), uses a geared transmission with a reduction mode which makes it suitable for climbing ramps. It also has a hill holding system which prevents the wheelchair from rolling backwards but the movement of the system is limited to the forward direction.

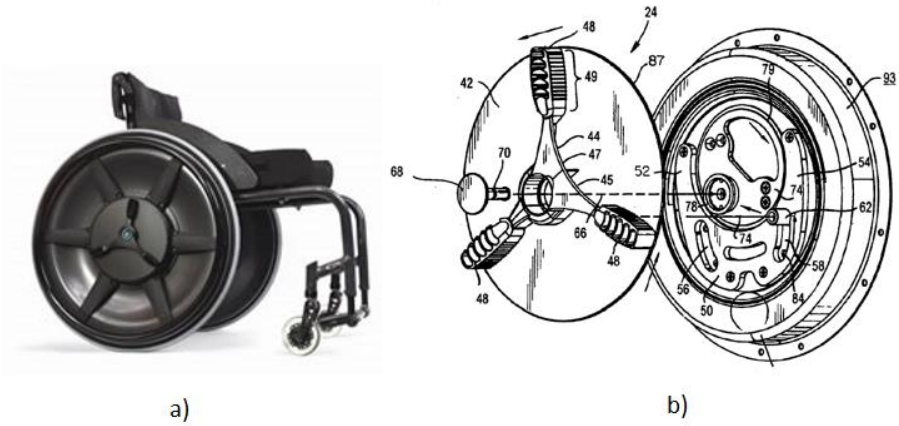

Fig. 12. a) View of the MagicWheels. b) Exploding view of the mechanism.

In this thesis, a propulsion geared system which can be attached to any manual wheelchair is proposed. The propulsion mechanism is fully mechanical and mainly

formed by a Planetary Gear Train with a self-locking capability which acts as a brake. The system is ideal for long ramps and helps reduce the effort needed over an extended period of time, preventing the user becoming fatigued, and allowing them to ascend or descend long ramps. Further, the propulsion system and the locking capability are properties which belong to the self-locking PGT. It is also suitable for any manual wheelchair and it is designed according to the physical condition of the subject.

Objectives

The aim of this thesis is to show two pioneering applications of Planetary Gear Trains with self-locking capability; a novel knee orthosis and a propulsion system for manual wheelchairs.

Firstly, a fully mechanical Stance-Control-Knee-Ankle-Foot-Orthosis that locks the knee during the stance phase of gait under any knee flexion angle and allows the flexion of the knee during the swing phase.

Secondly, a novel propulsion system for manual wheelchairs with self-locking capability when situated on ramps. This propulsion system can be adapted to any physical condition of the individual considering the input power that any user can hold. The system also locks itself when the user stops pushing the wheelchair.

The objectives for the making of the SCKAFO and the propulsion system for manual wheelchairs are as follows:

- Designing of the self-locking PGT adapting it to every application and determining elements that permit the functioning of the SCKAFO and the propulsion system.

- Validating the proposed design through the determination of the transmission ratio and the design conditions which need to be satisfied (i.e. constraints or meshing requirements).

- Constructing the proposed designs and adapting them to both healthy users and a standard wheelchair.

- Functional testing of the devices in order to validate the reliability and the behaviour of both devices.

Thesis content

The thesis consists of the compilation of two articles in which two new applications of Planetary Gear Trains with self-locking capability are shown. The first article has been published, the second has been accepted for publication:

- Jimenez GR, Salgado DR, Alonso FJ, del Castillo JM. *A new stance control knee orthosis using a self-locking mechanism based on a planetary gear train*. ASME. J. Mech. Des. 2018; doi:10.1115/1.4041780.

- Jimenez GR, Salgado DR, Alonso FJ, del Castillo JM. *A new manual wheelchair propulsion system with self-locking capability on ramps*, Mech. Sci., 9, 359-371, doi:10.5194/ms-9-359-2018, 2018.

Results and Discussion

The different applications proposed in this thesis are aimed at assisting the design of a fully mechanical SCKAFO and the design of a novel propulsion system with self-locking capability in manual wheelchairs. The results and further discussion of each device will be presented in the following paragraphs.

Stance-Control-Knee-Ankle-Foot-Orthosis

A new SCKAFO which can self-lock due to the actuation of a self-locking PGT has been built. The following steps show the construction of the orthosis:

- Design, evaluation and construction of a self-locking PGT with a transmission ratio of 1:12.
- Development of the three rods which complement the orthosis.
- Adaptation of the self-locking mechanism to a SCKAFO.
- Testing of the orthosis on two healthy subjects.

A two-stage Planetary Gear Train was built according to the equations proposed by [18] with a transmission ration of 1:12 and two multiplier stages were added in order to achieve a transmission ratio of 1:1 between the input and the output. Three rods were built and attached to the calf, the thigh and the output of the mechanism. The mission of the orthosis was to allow the motion during the swing phase of gait and self-lock during the stance phase. The rod attached to the output was also connected to the foot of the subject. During the stance phase, the contact with the ground produced a torque around the knee joint that locked the system and thus held the weight of the subject, allowing the user to continue walking. However, when contact with the ground (swing phase) was not made, the input of the system was done through the rod attached to the thigh, and so permitted the motion of the mechanism, allowing the user free swing until the contact with the ground was made again.

The SCKAFO was designed, built and tested on two healthy subjects in order to prove its functionality. The purpose of these trials was to demonstrate that the system self-locked during the stance phase, and allowed the user free swing during the swing phase.

The first trial was conducted on a healthy subject with 1.80 m of height and 80 kg of mass. The trial consisted of analysing the stance phase of the gait while walking at a preferred speed, and thus prove in a qualitative way that the device self-locked while load bearing. The trial proved that the orthosis permitted free swing during gait,

allowing the user to move the joint freely. In this trial the device self-locked at an 8-degree knee flexion angle during the stance phase, which was maintained until contact with the ground terminated.

The same trial was tested on a different subject with 70 kg of mass and 1.80 m of height. The knee flexion angle during the stance phase was approximately 1 degree which was maintained while there was contact with the ground. The purpose of this trial was to analyse the behaviour of the SCKAFO on a further subject with different gait patterns.

Finally, a third trial was tested on the second subject, who was told to intentionally change the gait pattern, imitating a crouch gait. The aim of this trial was to demonstrate that the system self-locked in the presence of a different knee flexion angle while load bearing. During the swing phase the angles were higher than in the other two trials. Before heel strike (system self-locks) there was an angle of 34 degrees which remained the same during the stance phase.

The three trials demonstrated that system can be adapted to the gait of any user as the limitation in flexion knee angle is not given by the orthosis but the subject itself. The main component of the system was a PGT, which allowed any angle to be reached between the input and the output of the system. It was also demonstrated that the orthosis can self-lock at any knee flexion angle during the stance phase of gait. The only requirement for the self-locking to appear is that there is contact with the ground. If there is not such contact, the joint is free to move, and any angle (regarding the limitations of the subject) can be reached.

Both subjects felt comfortable while load bearing and felt less muscle effort due to the self-locking characteristic of the device, even during abnormal gait. During the swing phase no issues arose and thus the user was able to bend the knee comfortably since the output of the device was not in contact with the ground.

Propulsion system for manual wheelchairs

A new propulsion system with self-locking capability for manual wheelchairs has been built. The following steps show the construction of the propulsion system:

- Design, evaluation and construction of a self-locking PGT with a transmission ratio of 1:12.
- Assembly of a new multiplier stage which permits a transmission ratio of 5:12.
- Adaptation of the propulsion system to a standard manual wheelchair.

To prove the reliability of a self-locking system in manual wheelchairs, a prototype of a propulsion system has been made. In order to achieve the self-locking capability, the tooth ratios were calculated according to the equations shown in [18]. In this application, the transmission ratio achieved was also 1/12 as it is the maximum transmission ratio that a PGT must have to achieve such self-locking capability. A multiplier stage was added to the output of the self-locking stage to attain the desired transmission ratio of 5/12. The transmission was mounted underneath the seat of a standard wheelchair as it was the most adequate place for the purposes of the project.

The housing of the mechanism is the fixed element and it is attached to the chassis of the wheelchair. An external pushrim was installed and connected to the input arm with the purpose of introducing power to the propulsion system and thus allowing the movement of the transmission.

The aim of this transmission is to allow the propulsion of the wheelchair when power is introduced by the external pushrim and also to self-lock when the power is introduced by the wheel. With this system the user does not need to activate or deactivate any external mechanism to brake the wheelchair when situated on a ramp. Furthermore, the effects of inertia when the user is on a ramp do not have to be overcome since the mechanism locks when power input is through the wheels.

The trials were conducted on a healthy subject with a height of 1.80m and a mass of 80 kg. The ramp used for the trials was located at the main entry of a residential area, it had a 10% slope and a length of 15 m. The first trial consisted of analysing the self-locking characteristic of the prototype.

The subject was told to remain stationary and not to move the external pushrim. While the subject was on the slope in an uphill direction the power input was transferred from the wheel to the output of the self-locking PGT, provoking the locking of the system and preventing the subject from rolling backwards. In the same way, when the subject was in a downhill direction, the prototype also self-locked. The subject was comfortable and did not feel any risk of rolling backwards or forwards while the prototype was locked. The first trial demonstrated that the system self-locked while the user was on a ramp without any power input.

The second trial consisted of introducing power through the external pushrim in order to test the motion of the prototype. By moving the external pushrim of the prototype, the power input was transferred from the external pushrim provoking the movement of the wheelchair. The subject was told to push the pushrim at the speed he considered appropriate. While pushing the wheelchair through various cycles and then halting the motion, the subject felt comfortable throughout the trial and did not feel at risk of rolling backwards or forwards. Further, the user did not feel the effects of inertia when changing between a stationary position and motion. This functioning prevented the user from rolling backwards while ascending or rolling downhill while descending. Further, the system moved while the power was introduced through the external rim allowing the user to ascend inclined ramps.

Conclusions

A new knee orthosis design encompassed within the group of SCKAFOs has been presented. It consisted of a locking system which permitted the movement of the limb during the swing phase and locked the knee joint during the stance phase. Three rods were placed on the lower limb, one of which was fixed to the thigh of the user. The second rod was connected to the calf and behaved as the input of the mechanism, allowing power to be introduced during the swing phase. The third rod was anchored to

the output of the mechanism and was responsible for introducing power through the output during the stance phase, and hence caused the locking of the mechanism as power could not be transmitted from the output.

Finally, it should be noted that unlike other orthoses designs proposed in the literature, this system is entirely mechanical. It therefore requires no electrical or electronic elements for its activation or deactivation. Additionally, it allows the knee to lock at any flexion angle during the stance phase and no torque is required to switch between the two phases of gait. These characteristics make this SCKAFO suitable for any subject, as the proposed design can be adapted to the gait of any user.

A new propulsion system used in manual wheelchairs to facilitate the ascending and descending on ramps was also designed and built. This transmission is based on a planetary gear train with self-locking capability. Due to the self-locking property, the transmission must be designed with a speed ratio lower than 1, making the device ideal for climbing ramps. The transmission is placed underneath the seat of the user, this allows that the chair maintains its dimensions regarding factors such as accessibility. The transmission shares both input and output axes which means that the system is coaxial. The input is connected to the new pushrim installed on a manual wheelchair and parallel to the wheel and its mission is to transmit power to the transmission. The output of the transmission is connected to the wheel. In this way, if the user introduces power through the new pushrim, the system will move the wheel. However, if the movement is introduced through the wheel, the system will self-lock due to the lack of power transmission in this direction. This system can be adapted to any physical condition (measured by the amount of power which each person can apply over a long period time) of the user. The transmission ratio is adapted to the physical condition of the user and the slope which is going to be ascended.

The system is formed by only mechanical components and no electronic or electrical actuator is required, it does not need any external elements for its activation/deactivation. This permits the user to push the wheelchair without fearing unexpected descending. These factors make this system suitable for every manual wheelchair user.

Finally, for future works, this type of self-locking transmission could have further applications in other types of vehicles such as bicycles and its usage could even be extended to transport and handling systems such as hoists. In the latter, the traditional transmission system could be modified with a self-locking PGT in order to lift heavy weights.

References

[1] Plooij, G. Mathijssen, P. Cherelle, D. Lefeber and B. Vanderborght, "Lock Your Robot: A Review of Locking Devices in Robotics," in IEEE Robotics & Automation Magazine, vol. 22, no. 1, pp. 106-117, March 2015. doi: 10.1109/MRA.2014.2381368.

[2] M. Controzzi, et al., Miniaturized non-back-drivable mechanism for robotic applications, Mech.Mach. Theory 10(10):1395-1406 doi: 10.1016/j.mechmachtheory.2010.05.008.

[3] C.M. Light, P.H. Chappell, Development of a lightweight and adaptable multiple-axis hand prosthesis, Medical Engineering & Physics 22 (2000) 679–684. DOI: https://doi.org/10.1016/S1350-4533(01)00017-0.

[4] M.C. Carrozza, G. Cappiello, S. Micera, B.B. Edin, L. Beccai, C. Cipriani, Design of a cybernetic hand for perception and action, Biological Cybernetics 95 (6) (2006) 629–644. DOI: 10.1007/s00422-006-0124-2.

[5] B. Massa, S. Roccella, M. C. Carrozza and P. Dario, "Design and development of an underactuated prosthetic hand," Proceedings 2002 IEEE International Conference on Robotics and Automation (Cat. No.02CH37292), Washington, DC, USA, 2002, pp. 3374-3379 vol.4. doi: 10.1109/ROBOT.2002.1014232

[6] N. Dechev, W.L. Cleghorn, S. Naumann, Multiple finger, passive adaptive grasp prosthetic hand, Mechanism and Machine Theory 36 (10) (2001) 1157–1173. doi: 10.1016/S0094-114X(01)00035-0.

[7] Wilian M. dos Santos, Glauco A.P. Caurin, Adriano A.G. Siqueira. Design and control of an active knee orthosis driven by a rotary Series Elastic Actuator Control Engineering Practice 58 (2017) 307–318. doi: 10.1016/j.conengprac.2015.09.008.

[8] Olivier, J., Ortlieb, A., Bouri, M., & Bleuler, H. (2015). Mechanisms for actuated assistive hip orthoses. Robotics and Autonomous Systems, 73, 59-67. DOI:10.1016/j.robot.2014.10.002.

[9] In, H., Kang, S., & Cho, K. (2012). Capstan brake: Passive brake for tendon-driven mechanism. 2012 IEEE/RSJ International Conference on Intelligent Robots and Systems, 2301-2306.

[10] Wolfrom, U., Der Wirkungsgrad von Planetengetrieben. Werkstatttechnik. 1912. p. 615-617.

[11] Loomann J. Zahnradgetriebe: Grundlagen, Konstruktionen, Anwendungen in Fahrzeugen. Springer Berlin Heidelberg: New York 1996.

[12] Müller HW. Die Umlaufgetriebe. Auslegung und vielseitige

[13] Athanassios Mihailidis and Ioannis Nerantzis, " A New System for Testing Gears Under Variable Torque and Speed", Recent Patents on Mechanical Engineering (2009) 2: 179. https://doi.org/10.2174/2212797610902030179.

[14] Cesaroni, A.F.: An imbricate type epicyclic reduction gear. Italy Pat. App. Publ. EP1396660A2, 2003.

[15] Butsch, M., Eisele, F., Fries, U.: Spielarmes Wolfrom-Planetenzahnradgetriebe, Germany Pat. App. Publ. EP0678688 A1, 1994.

[16] Orlowski, B.: Wolfrom-Planetenzahnradgetriebe mit axial in zwei unterschiedlich verzahnte Bereiche aufgeteilten Planetenrädern, Germany Pat. App. Publ. EP0627575 B1,1994.

[17] Schulz, H.: Planetengetriebe, Germany Pat. App. Publ 19928385, 2000.

[18] D.R. Salgado, J.M. del Castillo, Conditions for self-locking in planetary gear trains. J Mech Des Trans J. Mech. (2006) 960-968. doi:10.1115/1.2748449.

[19] Ikejo K, Nagamura K, Yada T, Kagari Y. Self-Locking of 2S-C Type Planetary Gear Train Composed of External Gears. ASME. International Design Engineering Technical Conferences and Computers and Information in Engineering Conference (2009) 39-46. doi:10.1115/DETC2009-86291.

[20] Jose M. del Castillo, The analytical expression of the efficiency of planetary gear trains, Mechanism and Machine Theory, Volume 37, Issue 2, 2002, Pages 197-214, ISSN 0094-114X, doi:10.1016/S0094-114X(01)00077-5.

[21] Karaivanov, D; Troha, S.; Pavlova, R. Investigation into self-locking planetary gear trains through the lever analogy. Transactions of FAMENA. 2012, Vol. 36 Issue 1, p13-24.

[22] Yakimovich, T., J. Kofman, and E. D. Lemaire. Engineering design review of stance-control knee-ankle-foot orthoses. Journal of Rehab Res and Dev. Vol 46, Number 2, 2009, 257-268. DOI: 10.1682/JRRD.2008.02.0024.

[23] Andrysek J, Leineweber MJ, Lee H. Development and Evaluation of a Mechanical Stance-Controlled Orthotic Knee Joint With Stance Flexion. ASME. J. Mech. Des. 2017;139(3):035001-035001-7. doi:10.1115/1.4035372.

[24] van der Woude LHV, Dallmeijer AJ, Janssen TWJ, et al: Alternative modes of manual wheelchair ambulation: An overview. Am J Phys Med Rehabil 2001;80:765–777.

[25] Babilas J., Automatic Wheel chair brake, United States App. Publ: 4,623,043, 1986.

[26] Dugas G.A, Automatic braking wheelchair, United States App. Publ: 5,984,334, 1999.

[27] Melvin G. Hector, Jr., Tucson, Structure, components and method for constructing and operating an automatically self locking manually propelled vehicle such asa wheel chair, United States App. Publ: US 8,622.409 B2, 2014.

[28] Meginniss, S. M. and SanFrancisco, A. S.: Two-Speed manual wheelchair wheel, United States Pat. Appl. Publ., 53, US 2006/0197302 A1, 2006.

Appendix

The main content of this thesis is based on the following journal papers.

- Jimenez GR, Salgado DR, Alonso FJ, del Castillo JM. *A new stance control knee orthosis using a self-locking mechanism based on a planetary gear train*. ASME. J. Mech. Des. 2018; doi:10.1115/1.4041780. (Accepted for publication)

- Jimenez GR, Salgado DR, Alonso FJ, del Castillo JM. *A new manual wheelchair propulsion system with self-locking capability on ramps*, Mech. Sci., 9, 359-371, doi:10.5194/ms-9-359-2018, 2018. (Published)

A complete copy of each paper is shown in the following pages.

A new stance control knee orthosis using a self-locking mechanism based on a planetary gear train

G. R. Jiménez[1], D. R. Salgado[1], F. J. Alonso[1], J.M. del Castillo[2]
[1]Department of Mechanical, Energy and Materials Engineering. University of Extremadura.
gaspar.rodriguez.jimenez@gmail.com; {drs, fjas}@unex.es
[2]Department of Material Science and Transportation Engineering. University of Seville.; delcastillo@us.es

Abstract

The objective of this work was to design and build a fully mechanical knee orthosis. A knee orthosis should both allow control of the angle of flexion of the knee during the stance phase of the gait cycle and leave the joint free during the swing phase. Knee orthoses are normally used to assist the walking of people suffering from muscle weaknesses or gait pathologies in order to avoid excessive knee flexion during the stance phase. The design of the orthosis proposed in the present work is characterized by allowing the knee to be locked at any angle of flexion during the stance phase, and because the orthosis can be unlocked to allow the joint to be released in the swing phase without the action of any external agent, i.e., without requiring external electrical or electronic systems for the control and performance of the orthosis. These characteristics mean that the design can be adapted to the gait of any user. The proposed design consists of a set of three rods, one attached to the user's thigh, another to the calf, and the other to the foot, connected to each other by a self-locking planetary gear train (PGT). [DOI: 10.1115/1.4041780]

Keywords: orthoses; rehabilitation engineering; knee locking system; self-locking planetary gear train; stance control.

1. Introduction

There are numerous potential causes of muscle weakness. These include post-polio syndrome, spinal cord injury, trauma, multiple sclerosis, muscular dystrophy, unilateral leg paralysis, and paresis [1]. Sufferers usually need a passive or active orthosis to help them lock the knee while walking. Many of the orthoses currently available on the market are mainly used in rehabilitation [2-5] or to improve control of the ankle joint [6-8] or knee [9-14]. They can be classified into three distinct groups: passive knee-ankle-foot-orthoses (KAFOs), stance control KAFOs (SCKAFOs), and dynamic KAFOs.

Passive KAFOs act without any external power source. Most of them lock the knee during both the stance and the swing phases. The knee remains blocked resulting in an uncomfortable gait requiring high energy consumption [1] on the user's part. This leads many of these patients (more than 60%) to stop using them [12]. There are various types of locking systems used in these orthoses: ratchet lock, drop lock, bail lock, and dial lock. However, they all have the disadvantage that they can not be locked at any, not predetermined, angle of flexion [11], i.e., they only allow blockage in certain joint positions, which makes their use less comfortable and less adaptable to each user.

The second group, SCKAFOs, are orthoses that lock the knee during the stance phase and allow knee flexion during the swing phase of gait. Not all SCKAFOs block at any angle of knee flexion, and those that do, such as the Quasi-Passive Compliant Stance Control Knee-Ankle-Foot Orthosis [12], use sensors to electronically control their action. These orthoses improve gait control relative to passive KAFOs. In addition, they can reduce gait compensations and

allow patients to walk with less effort [1]. They have been studied and improved extensively due to their great reliability. There remain, however, certain abnormal patterns during gait due to knee blockage in the stance phase [11]. They use a great diversity of locking mechanisms. Some examples are ratchets, cams, friction mechanisms, hydraulic mechanisms, and magnetically activated clutches. The orthosis proposed in the present paper belongs to the SCKAFO family because the control of gait is established in the stance phase, and released during the swing phase.

Dynamic KAFOs reproduce the user's normal gait more accurately than the foregoing orthoses since they implement a system of control of the different moments/movements that constitute the various phases of gait. They allow the knee to be locked at any flexion angle during gait, and hence allow control of the complete gait cycle whether in the stance phase or in the swing phase. They are bulkier than other orthoses because they necessarily require a sensor, actuation, and control system and a battery. Different types of mechanisms are implemented to perform the blocking during the stance phase. These include spring mechanisms [13], a pneumatic system [14], a hydraulic system [11], and a combination of superelastic rods and springs [11]. Although orthoses of this type can simulate gait correctly, they are not completely mechanical solutions like the one proposed here. Moreover, their complex control system means that they are mainly used as laboratory rehabilitation devices [11].

The orthosis proposed here is characterized by allowing the knee to be locked at any flexion/extension angle during the stance phase, and because it can be unlocked to release the joint in the swing phase without the action of any external agent, i.e., without requiring external electrical or electronic systems. It is therefore a fully mechanical design, classifiable as an SCKAFO as indicated above.

The objective of the present work was to design and build a new SCKAFO type knee orthosis that adapts adequately to any user's gait, regardless of the angle of flexion during stance. It requires no external control system. Instead, control is carried out directly in response to the user's own movements, as we shall detail below. The design consists of a set of three rods or bars, one attached to the thigh, one to the calf, and one to the foot, connected to each other by a self-locking planetary gear train (PGT).

The paper is organized as follows. Section 2 describes the locking mechanisms used. Section 3 presents the design of the proposed mechanical SCKAFO based on a self-locking PGT. Section 4 the validation of the proposed design and Section 5 shows the functional and qualitative evaluation of the device. Finally, Section 6 presents the conclusions and future works.

2. Locking mechanisms used in orthoses design

There are various knee locking systems, whether for control in the stance phase, in the swing phase, or both. However, very few of them are fully mechanical, i.e., not requiring sensors, actuators, electrical systems, etc. In the present work, only mechanical locking systems that do not require any type of actuation are analysed. In particular, we shall not include the blocking mechanisms of Dynamic KAFOs. The following are some of the mechanisms implemented in Passive KAFOs and SCKAFOs.

Fig. 1 shows a ratchet lock system used in a Passive KAFO. This system does not allow knee

locking in all positions. It is used to facilitate the patient's standing from a sitting position to an upright position. To this end, the mechanism has a locking system that varies every 12° until the full extension of the knee, thus avoiding knee flexion. To unlock the system (flex the knee), it is necessary to manually press a lever.

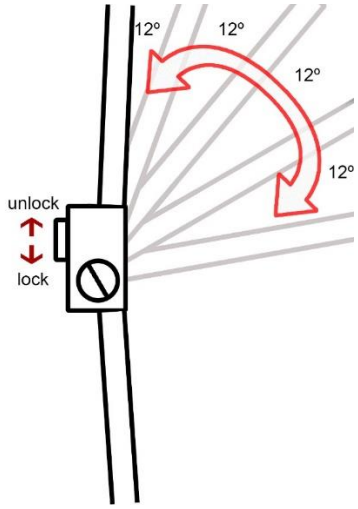

Fig. 1. Ratchet lock locking mechanism.

The dial lock mechanism shown in Fig. 2 is another example of a locking mechanism used in the design of Passive KAFOs. This system only allows a pre-configured locking position. By using a dial, the subject can choose the desired locking position, and the system will then allow knee flexion to the chosen angle. This type of mechanism is most frequently used for rehabilitation.

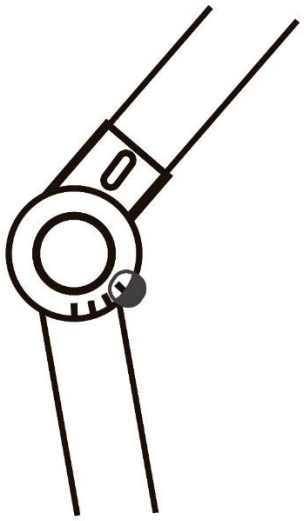

Fig. 2. Locking system based on a dial lock.

Fig. 3 shows the Ottobock Bock Free Walk System created by Becker Orthopædic UTX [15]. This system allows free flexion of the knee during the swing phase, and completely blocks the knee during the stance phase. It remains locked unless the ankle produces a dorsiflexion of 10°. At this point, the locking system disengages and the knee can again move freely during the

swing phase.

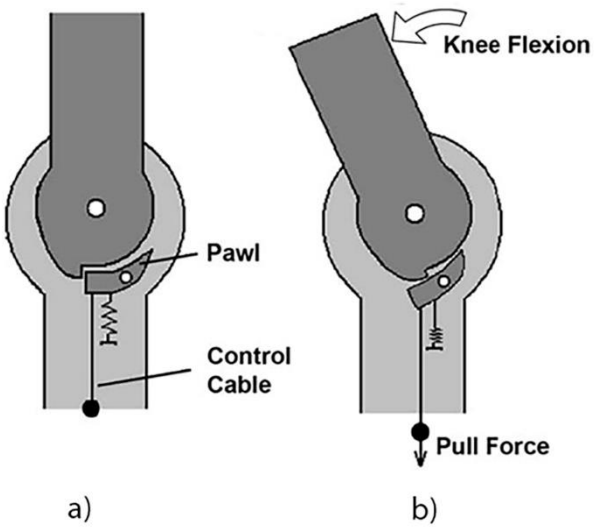

Fig. 3. Ottobock Free Walk/Becker Orthopædic UTX. Spring loaded mechanism. Image obtained from [19]

Fig. 4 shows the Fillauer Swing KAFO system [15]. This employs a mechanical locking system in which a pawl moves under gravity. This device locks the knee during the stance phase and the knee moves freely during the swing phase. It locks in full extension of the knee, so that there is only one locking position. Release does not occur automatically but depends on the angle of hip flexion. Fig. 4(a) shows the behaviour of the system under complete knee extension when the thigh is anterior to the individual's body, and Fig. 4(b) when the thigh is posterior to the body, when the pawl falls out of engagement.

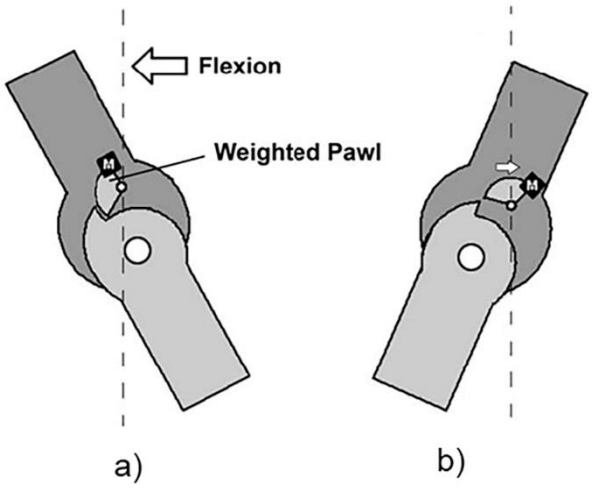

Fig. 4. Fillauer swing KAFO [19] showing the behaviour of the orthosis in different situations.

Another locking solution is belt-clamping [15] (Fig. 5(a)). This system works by friction. The belt attaches to the upper and lower supports and extends through the knee shaft. The resulting flexural strength increases as the knee flexes [16] allowing locking of the knee joint.

The tension decreases with extension of the knee at any time. This system requires rods along the medial and lateral zones of the leg to operate (Fig. 5(b)).

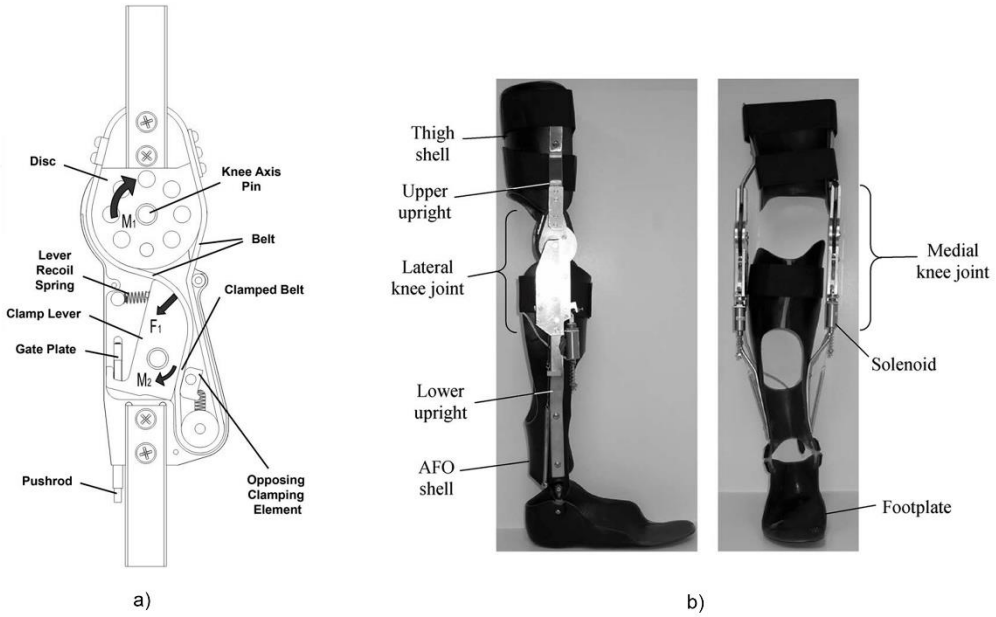

Fig. 5. Belt-Clamping SCKAFO. a) Components of the SCKAFO. b) Two views of the orthosis. Image obtained from [20].

The various mechanical locking systems currently used in orthotic design are summarized in Table 1. The last row of the table corresponds to the locking mechanism of our proposed new orthosis design.

Table 1.
Characteristics of mechanical locking systems in orthoses.

Name	Type	Condition of the knee joint during the gait cycle	Locking Position	Unlocking mechanism
Ratchet lock	Passive KAFO	The knee extends freely but flexion is blocked during the entire gait cycle	Every 12 degrees until full extension	Knee flexion is blocked automatically due to the ratchet lock. The knee is unlocked by pressing down the release lever of the ratchet lock
Dial lock	Passive KAFO	The knee is locked during the entire gait cycle	At any specified knee flexion angle	The knee locks automatically when extending. It is unlocked by pulling up the dial of the KAFO
Otto Bock Free Walk Becker Orthopaedic UTX.	SCKAFO	The knee is locked in stance and moves freely in swing	Full extension	10 degrees ankle Dorsiflexion to pull down And disengage the lock
Fillauer swing KAFO	SCKAFO	The knee is locked in stance and moves freely in swing	From 0 to 10 degrees of knee flexion	Automatically
Belt-clamping	SCKAFO	The knee is locked in stance and moves freely in swing	Any knee flexion angle at heel strike	Automatically
Proposed knee-locking system	***SCKAFO***	***The knee is locked in stance and moves freely in swing***	***Any knee flexion angle at foot strike***	***Automatically***

All of the mechanisms discussed above except the one proposed in this paper require an unlocking torque for the transition between the locked and the unlocked phases. In the mechanism proposed in this work, unlocking occurs automatically, and the patient does not need to perform any extra movement to disable the block during the stance phase. They simply have to maintain their own walking pattern for the correct functioning of the orthosis. In addition, the locking occurs at any knee flexion angle, and does not need any part that affects the mechanism in the medial zone of the leg. In the following, we shall divide our explanation of the design into three parts. First, we shall describe the proposed blocking mechanism, explaining how the system is arranged for its proper operation. Second, we shall discuss the different possible construction solutions and the tooth ratios needed for self-locking to occur. Third, a dynamic analysis will be included to verify the viability of the chosen solution. And fourth, a qualitative study of a prototype built will be tested on a healthy subject to analyse the self-locking condition.

3. Design of the orthosis based on a self-locking Planetary Gear Train

The proposed orthosis design consists of two parts: a locking system based on a self-locking planetary gear train, and a set of three rods or bars. Each of these rods has a specific function, and is attached to one member of the PGT and to different parts of the leg. In particular, one rod is attached to the thigh (Rod 1), another to the calf (Rod 2), and the other to the foot (Rod 3). They are connected to each other by a self-locking planetary gear train. An outline of this design is shown in Fig. 6.

As can be seen in the Fig. 6(a), Rod 1 is attached to the thigh, and is anchored in position to the PGT's housing, i.e., to the fixed member of that transmission (see Fig. 6(c)). Rods 2 and 3 are attached to the PGT's input and output axes.

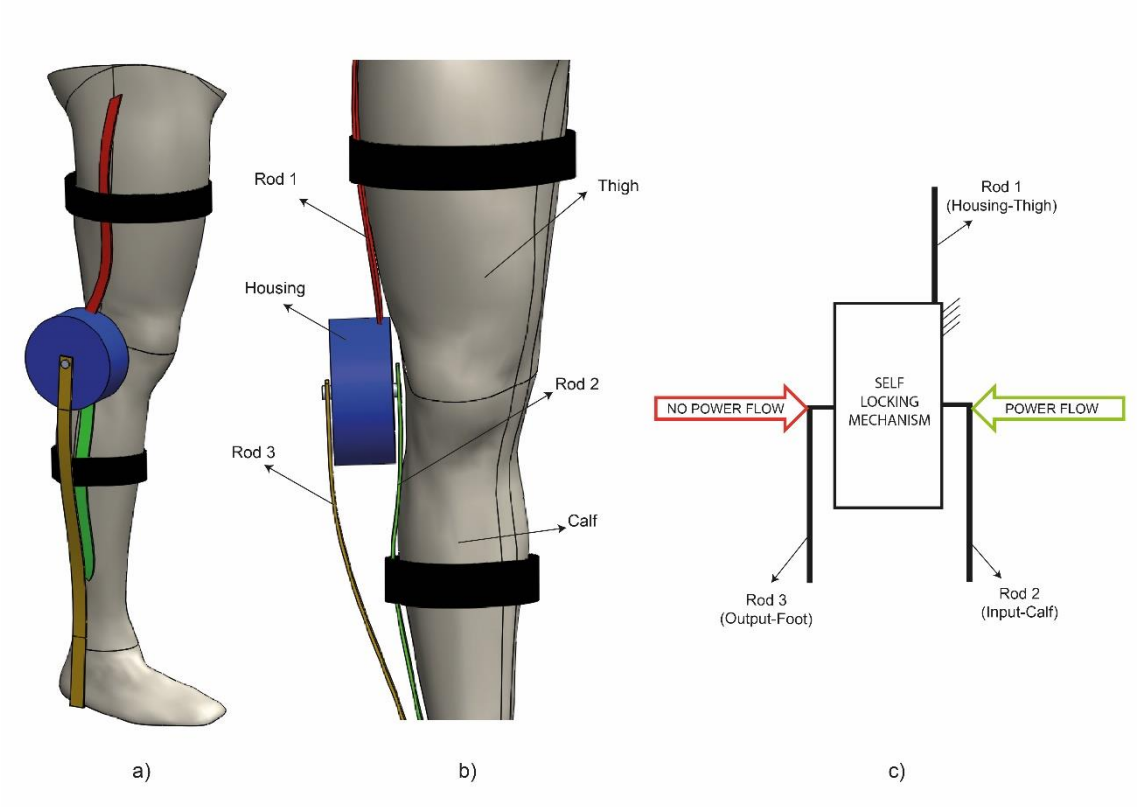

Fig. 6. a) and b) Two views of the solution for the construction of the SCKAFO design (rods and self-locking mechanism in relation to the limb). c) Schematic diagram of the proposed SCKAFO design.

The task of Rod 1 is to support the orthosis, and to serve as the element establishing the fixed member of the transmission, i.e., the member whose angular velocity with respect to the thigh is zero. Rod 2 is attached to the calf and the PGT's input. It is this rod which allows power to be input during the swing phase, i.e., when the system is not blocked. Rod 3 is connected to the PGT's output. Its mission is to allow the orthosis to block during the stance phase when the foot comes into contact with the ground. This is because power input to the transmission in the stance phase is through this rod, and in this sense the transmission does not let power flow towards Rod 2, so it is self-locking by causing Rods 1 and 3 to be fixed in place in this phase of the gait cycle. The knee locking system implemented in this design allows the knee to flex and to extend during the swing phase regardless of the angle of flexion of the knee.

Fig. 7 shows how the locking mechanism acts during gait. At the beginning of the gait cycle, the foot (Rod 3) makes contact with the ground (initial contact). As a result of this, a reaction occurs which results in a resistant torque (To) in the knee that impedes the knee's flexion. This torque is produced at the output of the mechanical device (Rod 3), and causes the PGT to self-lock when attempting to send power from Rod 3 to Rod 2. Thus, the knee remains locked during the sub-phases of stance, i.e., loading response, mid stance, terminal stance, and pre-swing (see Fig. 7) since the position of Rod 3 relative to Rod 1 stays fixed. When the user enters the swing phase in the initial swing, there is no longer any contact with the ground. So the input torque on the locking mechanism, Ti, is produced by the rotation of the calf (Rod 2) with respect to the thigh (Rod 1). This torque causes power flow in the PGT to be from Rod 2 to Rod 3, i.e., in the direction for which the PGT does not self-lock and therefore allows movement. In particular, the transmission allows the movement Rod 3 in phase with Rod 2 during mid swing and terminal swing, until the foot again comes into contact with the ground, and the cycle is repeated.

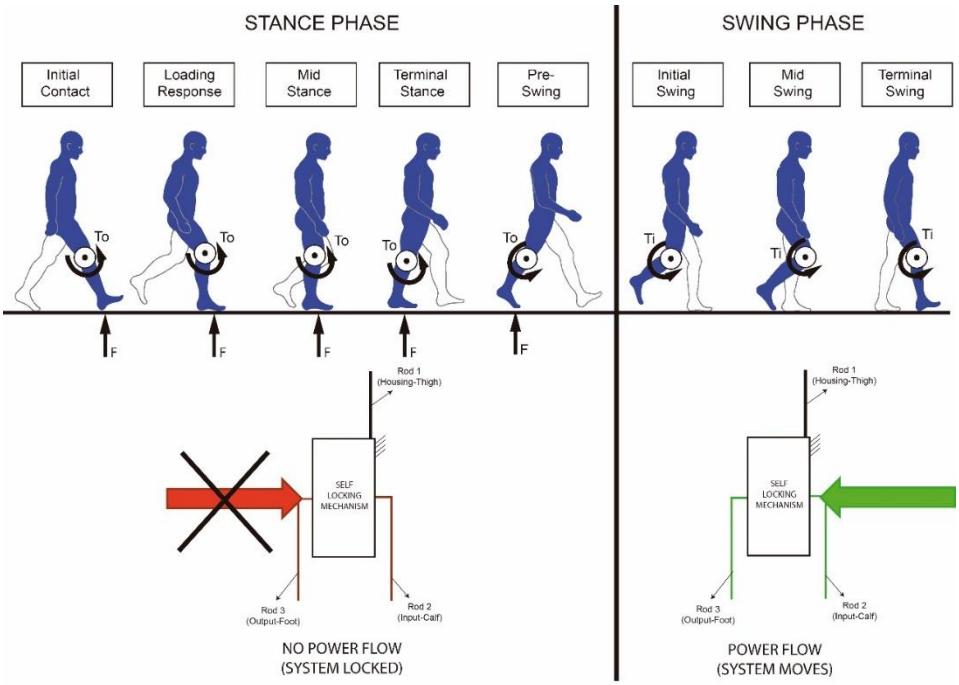

Fig. 7. Performance of the knee locking system during different stages of gait.

With respect to the design of the transmission implemented in the orthosis, in the swing phase, Rods 2 and 3 need to have the same angular velocity relative to the fixed member (thigh), and therefore the design must have a transmission ratio equal to unity. However, it has been shown [16] that the transmission ratio of a self-locking PGT has to be less than unity, i.e., it has to be designed as a speed reducer. Therefore, in order to obtain a transmission ratio of unity between Rods 2 and 3 of the orthosis, it is necessary to include another planetary transmission in series with the self-locking PGT that multiplies the speed so as to obtain a final transmission ratio equal to unity. Fig. 8 is a schematic diagram of such an orthotic locking system consisting of a speed reducer self-locking PGT with a speed multiplier PGT that can result in an overall transmission ratio of unity.

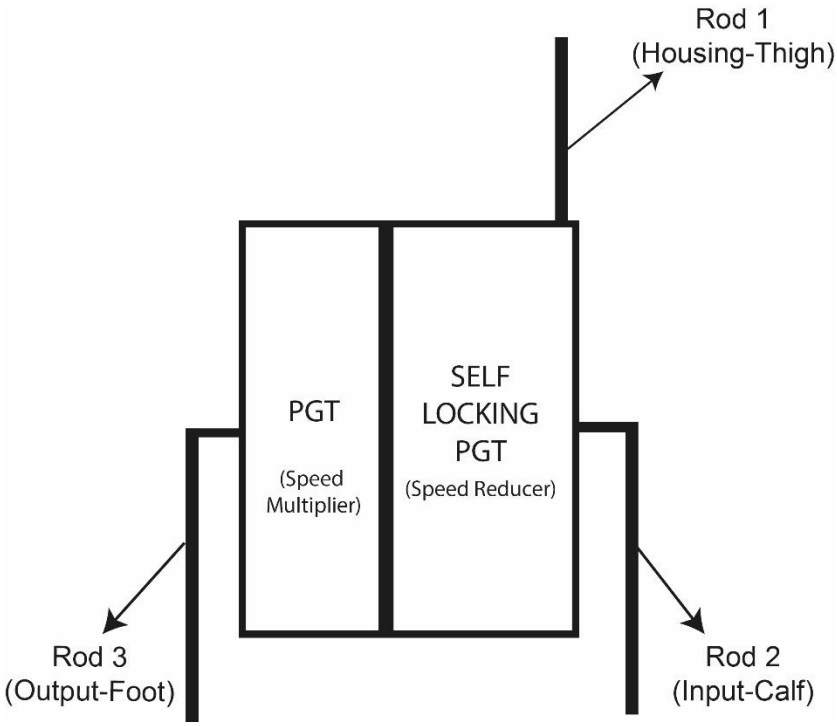

Fig. 8. Parts of the knee locking system.

4. Validation of the proposed orthosis design

In this section a solution will be determined for the construction of the proposed orthosis, in particular, for the knee locking system shown in Fig. 8. For a PGT to be self-locking, it must satisfy a series of design conditions that allow only a reduced set of constructional solutions [16].

For simplicity of construction, we considered the two 4-member self-locking PGT solutions, since these have the fewest members. These two solutions are shown in Fig. 9. We chose to analyse the one shown in Fig. 9(a) because it has external (gear/gear) pairs rather than internal (gear/ring-gear) pairs. For this solution to be self-locking, the following expression must be satisfied:

$$\eta_{14}\eta_{24} < \frac{Z_{24}}{Z_{14}} < \frac{1}{\eta_{14}\eta_{24}} \tag{1}$$

where η_{ij} is the ordinary efficiencies of the circuits of the PGT. The ordinary efficiency is the efficiency of the gear pair if the arm linked to the planet were fixed. By means of this efficiency, one introduces into the overall efficiency calculation of the gear train the friction

losses that take place in each gear pair. Although the value of the ordinary efficiency in each gear pair depends on the number of teeth of its gears, on the operating conditions (applied torque, speed, lubricant type and method, temperature), and on geometric factors such as the approach portion and the recess portion and on tooth surface roughness [17-19], for the analysis of the self-locking conditions; it is sufficient to consider a value of the ordinary efficiencies slightly less than unity [16]. In Eq. (1) Z_{ij} is the tooth ratio of the gear pair formed by the linking members *i* and *j*. In particular, Z_{ij} is defined as Z_{ij}=Z_i/Z_j. For the definition of the tooth ratios to satisfy the Willis equations, Z_{ij} must be positive if the gear is external (meshing gear–gear) and negative if it is internal (meshing ring gear–gear). For the train of Fig. 9(a), one would have to take $Z_{14} > 0$ and $Z_{24} > 0$.

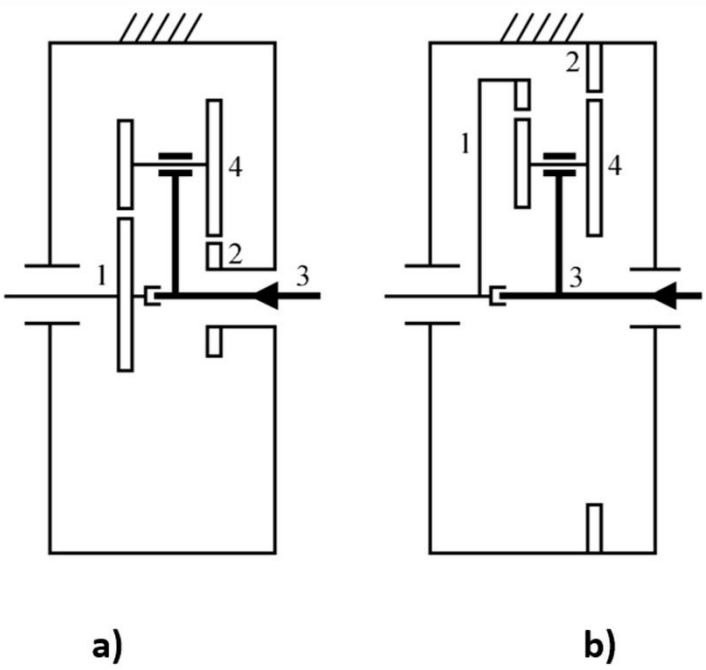

Fig. 9. Constructional solutions for 4-member planetary gear trains.

The two solutions for a 4-member self-locking PGT shown in Fig. 9 only allow power flow with input through the arm (Member 3) and output through the sun (Member 1), as indicated by the arrow in the Fig. 9. The transmission ratio of such 4-member PGTs with arm input is [20]:

$$r = \frac{Z_{14}-Z_{24}}{Z_{14}} \tag{2}$$

The constraints on the design of an orthotic locking system based on PGTs can be grouped into those involving size and geometry, as will be and those involving meshing requirements. These two groups will be detailed below.

Constraints involving gear size and geometry

The first constraint is a practical limitation of the range for the acceptable face width *b*. This constraint is as follows:

$$9m < b < 14m \tag{3}$$

Where m is the module of the gear. All of the kinematic and dynamic parameters of the transmission depend on the values of the tooth ratios Z_{ij}. In theory, the tooth ratios can take any value, but in practice, they are limited mainly for technical reasons because of the difficulty in assembling gears outside of a certain range of tooth ratios. In this work, the tooth ratio for the design of mechanical spindle speeders are quite close to the recommendations of Müller [17] and the American Gear Manufacturers Association (AGMA) norm [20], and are:

$$0.2 < Z_{ij} < 5 \tag{4}$$

$$-7 < Z_{ij} < -2.2 \tag{5}$$

with the constraint given by Eq. (4) being for external gears and that by Eq. (5) for internal gears. It is important to note that these constraints are valid for designs with different numbers of planets (*Np*) [17].

Another constraint that will be imposed on the design of four-PGT with double planets, as the self-locking PGT implemented in the orthosis design, is that the ratio of the diameters of the gears constituting a double planet [20] is shown in the below equation:

$$\frac{1}{3} < \frac{d_4}{d_{4'}} < 3 \tag{6}$$

where d_4 and $d_{4'}$ are the diameter of the gears than constitutes the planet gear that meshes with members 1 and 2 (see Fig. 9).

Planetary gear train meshing requirements

The meshing requirements are given by the AGMA norm [20]. For planetary systems with double planets must, either of which, factorise with the number of planets in the sense of Eq. 7 below (see AGMA norm [20]):

$$\frac{Z_2P_2 \pm Z_1P_1}{N_p} = an\ integer \tag{7}$$

where P_1 and P_2 are the numerator and denominator of the irreducible fraction equivalent to the fraction $Z_{4'}/Z_4$; where $Z_{4'}$ is the number of teeth of the planet gear that meshes with member *1* and Z_4 is the number of teeth of the planet gear that meshes with member *2* (see Fig. 9):

$$\frac{Z_{4'}}{Z_4} = \frac{P_1}{P_2} \tag{8}$$

In order to satisfy the above requirements, and since the 4-member PGT with an input arm is a reduction transmission, the maximum transmission ratio that can be achieved in order to obtain a self-locking train, i.e., Eq. 1, and which also satisfies the above conditions (Eqs. (2-8)), is $r = 1/12$. This maximum possible transmission ratio was chosen since, as indicated previously, the transmission ratio between Rods 2 and 3 must be unity, and hence less multiplication will need to be implemented at a later stage.

As a specific design proposal, we propose the following teeth numbers for the self-locking PGT of Fig. 9(a):

$Z_1 = 21 \quad Z_2 = 21 \quad Z_4 = 24 \quad Z_{4'} = 22$

and a planet composed of three gears (Np = 3), as shown in Fig. 10.

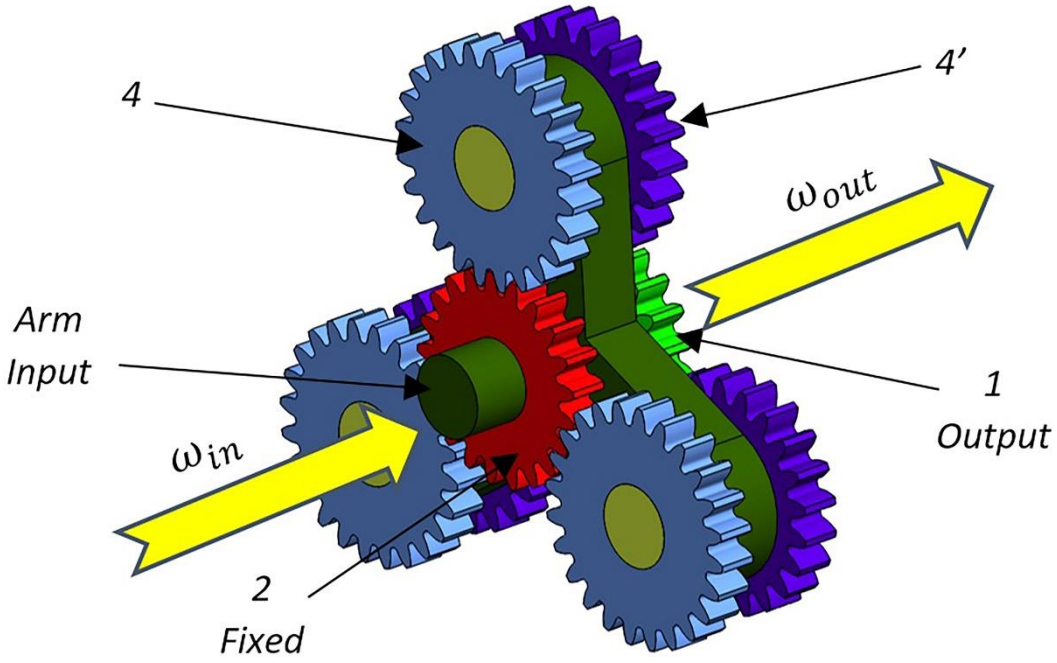

Fig. 10. Assembly of the self-locking PGT. The arrows of ωin and ωout represent the direction in which the PGT transmits power.

For the speed multiplier, we chose a two-stage design because, as will be explained below, the transmission will have to bear high loads, and a single stage multiplier would mean that the complete mechanism would be of a larger diameter. The two multipliers implemented are of ×3 and ×4 multiplication ratios (Fig. 11(a)).

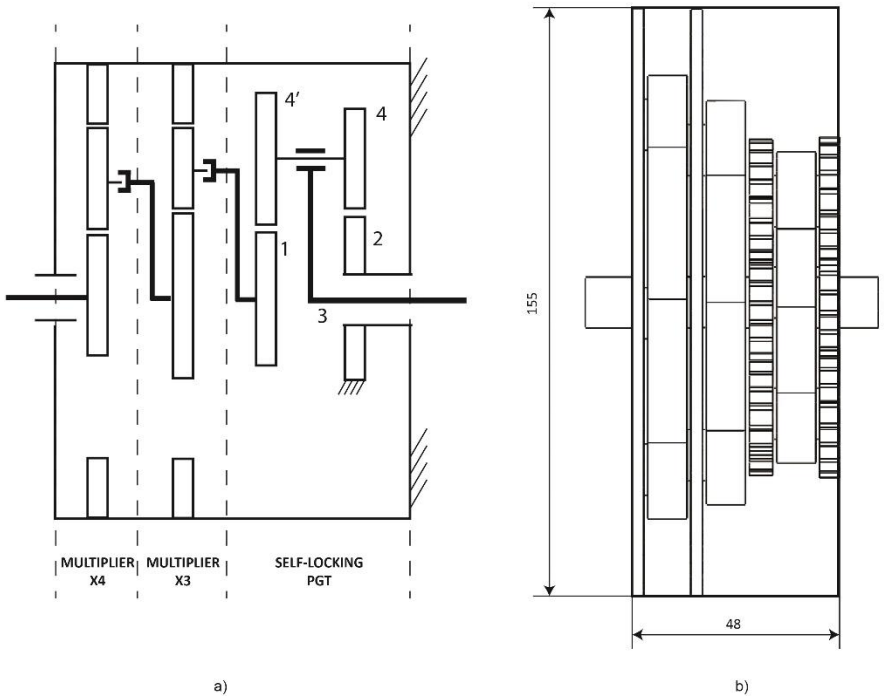

Fig. 11. a) A scheme of the complete transmission mechanism implemented between Rods 2 and 3 of the orthosis. b) Dimensions (in mm) of the mechanism (for a person of 80 kg mass, the knee supports 52 Nm).

To size the transmission mechanism between Rods 2 and 3 of the orthosis, we determined the torques that the system must support during the stance and swing phases.

In the stance phase, the torque transmitted to the transmission is the knee-locking torque required to prevent thigh-calf flexion and that is triggered by a reaction force at the initiation of that phase. In the literature, this torque is clearly defined for the gait cycle [11, 14], and depends on the subject's weight. One sees in Fig. 12 that the maximum torque produced in the knee during the stance phase is approximately 0.65 Nm/kg. Hence, for an average person of 80 kg mass, the knee supports 52 Nm.

During the swing phase, the torques produced in the knee are smaller than during the stance phase. Power recirculation occurs when the power that is transmitted by a gear pair is greater than the input power. This phenomenon appears in self-locking PGT [16]. However, as can be seen in Fig. 12 the torques produced around the knee during the swing phase are very low compared to the stance phase, so this phenomenon does not significantly affect the device. Even in these cases, however, because the power that the subject inputs in the swing phase is relatively low, the torques that the gears must support are smaller than in the stance phase. The torques in the swing phase were calculated using the expressions given in Refs. [16] and [21]. In sum therefore, the locking system must be designed to withstand the stresses that occur during the stance phase, since this is the more restrictive.

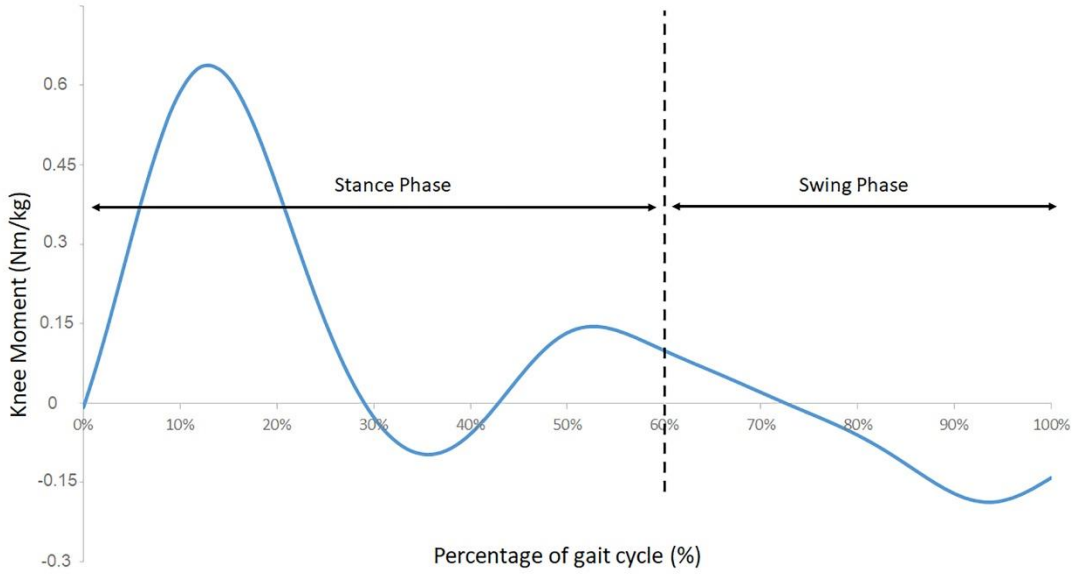

Fig. 12. Knee torques during a gait cycle.

The representation of the dynamic loads on the cogs of the gears was calculated using CAE tools. It is very difficult with this type of tool to calculate the power recirculation that occurs in the self-locking PGT when the system is in motion. As noted above, however, the stage with the greatest torques in the gears is when the mechanism is blocked in the stance phase. Table 2 lists the characteristics of the gears in the complete self-locking PGT and planetary multiplier system.

Table 2.

Characteristics of all the gears that form the self-locking PGT with the multipliers. r_p: pitch radius in mm, r_a: addendum radius in mm, r_d: deddendum radius in mm, α: pressure angle, m: module in mm, t: thickness in mm, R_c: Ratio contact (x3) Due to the number of planets.

Member		Teeth	Distance Centres (mm)	r_p (mm)	r_a (mm)	r_d (mm)	α	m (mm)	t (mm)	R_c (x3)
Self-locking PGT	2	21	32.25	15.01	16.44	13.58	20	1.43	6	1.58
	4	24		17.16	18.59	15.73		1.43		
	1	21		15.75	17.25	14.25		1.5	6	1.57
	4'	22		16.5	18	15		1.5		
Multiplier x3	Ring	80	51	68	66.7	69.7	20	1.7	3	4.47
	Planet	40		34	35.7	32.3		1.7		1.63
	Sun	20		17	18.7	15.3		1.7		
Multiplier x4	Ring	90	45	67.5	66	69	20	1.5	3	5.39
	Planet	30		22.5	24	21		1.5		1.65
	Sun	30		22.5	24	21		1.5		

The housing in which the self-locking system is located is made of plastic. This material will hold the produced efforts due to the self-locking and will not affect in excess the weight of the device. The gears are made of steel with an elastic limit σ =241.27MPa. The rods are made of duraluminum. The torque produced by the locking of the system is known and fixed for each individual's gait, and must be supported by the complete system. This allows the locking system to be designed with acceptable dimensions taking the stresses between the cogs in contact into account. The contact ratios between the pairs of gears are high, and will allow the forces to be distributed over more points of contact, with consequently lower tangential forces on each zone of contact. From the data in Table 2, one sees that the suns (1 and 2) are the members of the PGT with smallest radii. Planets 4 and 40, forming the same member, share the supported torque between the two of them.

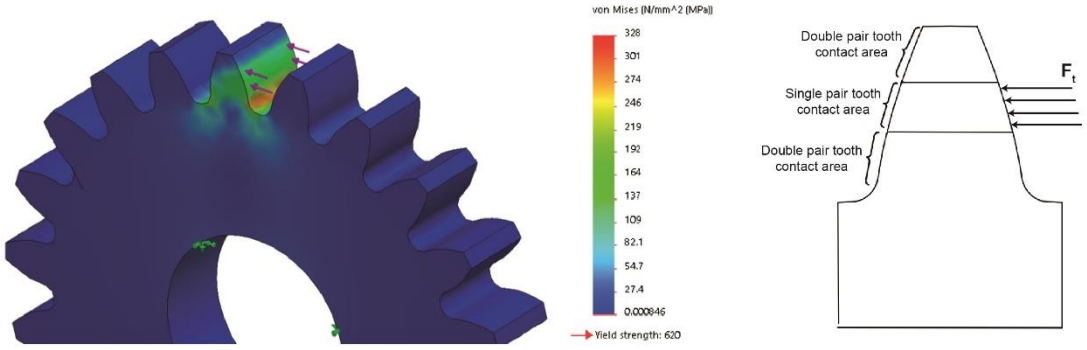

Fig. 13. a) Stresses produced by the tangential forces applied to the cog during the blocking phase. b) Areas in which the different contacts occur, and the application of the tangential force produced by the contact in the least favourable area.

Thus, the input and output members (1 and 2) of the self-locking PGT will be those that bear the most load. The method used to calculate the resistance of the mechanism is that described

in Refs. [21–24]. In particular, as illustrated in Fig. 13(a) for gear 2, the contact between two gears was simulated applying the tangential force caused by the torque to the center of the gear at the primitive radius, distributed over the thickness of the cog. Regarding the boundary conditions the gear is fixed in the center simulating the self-locking condition. The contact force is simulated as shown in Fig. 13(b). The results showed that the teeth of the gear indeed support the stresses generated. The different parts of the locking mechanism and their approximate dimensions that will allow the stresses produced during the stance phase to be supported are shown in Fig. 11(b). The length of the arms that connect the different stages of the mechanism was taken to be 10mm. All the elements designed in the knee lock system are straightcut gears. The mechanism's volume could be reduced if gears were used since the contact ratio between each gear pair would be greater, and hence the forces would be distributed over more points of contact. We decided to use straight cut gears for the present work because the speeds to which the system will be subjected are not high, and the manufacturing costs would be lower.

5. Functional and qualitative evaluation

In this work a prototype of the SCKAFO has been tested in order to validate the reliability and the behaviour of the device during the stance phase of gait. For the purpose of the trial, the prototype was built using medial and lateral support for both Rods 1 and 2. The third bar (Rod 3) was built in aluminum and attached to the output of the device. An insole was fixed to Rod 3 and its goal is to make contact with the ground. In Fig. 14, the complete proposed device is shown in a) front view and b) sagittal view.

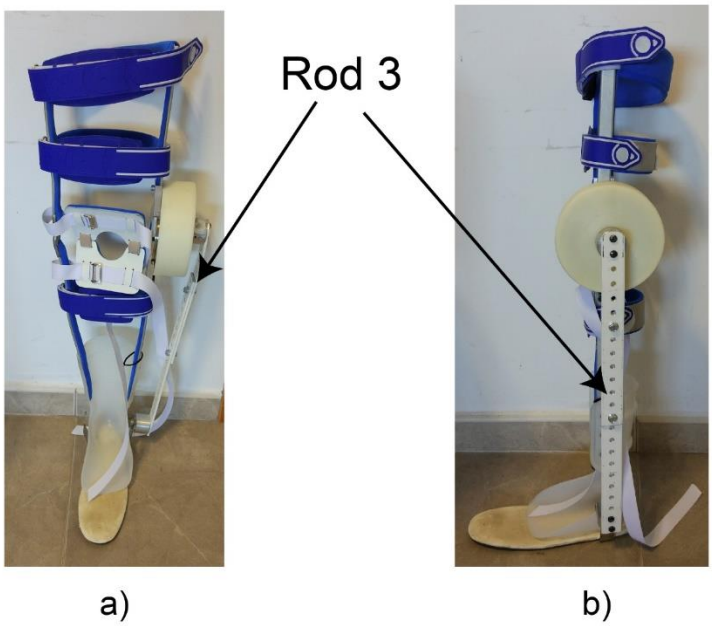

Fig. 14. a) Front view of the prototype built. b) Sagital view.

The first trial was conducted on a healthy subject with 1.80 m of height and 80 kg of mass (subject1). It consisted of analysing the stance phase of the gait while walking at a preferred speed, and prove in a qualitative way that the device self-locks while load bearing. Fig. 15 (a) shows different stages of gait during the stance phase and the swing phase.

The second trial was conducted on a new healthy subject with 70 kg of mass and 1.80 m of height (subject 2). Following the considerations of the previous trial, an analysis of the behavior of the orthosis was carried out in another subject.

The third trial (Fig. 15(c)) was analyzed on subject 2. In this case, the subject was told to maintain the knee flexion in order to imitate the crouch gait. The purpose of this trial is to demonstrate that the system self-locks in the presence of a different knee flexion angle while foot contact.

Being the main component of the device a self-locking PGT, any angle can be achieved between the input–output (rod 2–rod 3) and the fixed member (rod 1). The system adapts to any user's gait and the limitation in angle will be given by the gait limitation of the user. In Fig. 15 the knee angles during gait are shown for every subject. To measure the knee angle during both stance and swing phase, two lines were traced on the photograms of Fig. 15 representing rod 1 and rod 3 and the angle between these lines was calculated. During the swing phase two photograms of the cycle for each trials are shown, which represent initial swing and terminal swing, respectively. Variable a represents the angle between rod 1 and rod 3. During the stance phase, three photo grams of the cycle are shown.

It is evident that during the stance phase in all of the trials, the relative angle between rods 2-3 and rod 1 remains the same since there is a force contact with the ground, and under this condition the device is locked. However, when the contact with the ground finishes, the joint is free to move and the flexion of the knee occurs.

Fig. 15. Testing of the device on two healthy subjects: (a) normal cycle of gait on subject 1, (b) normal cycle of gait of subject 2, and (c) simulated crouch gait of subject 2

Different repetitions of every trial consisting of three or four steps for every gait cycle were carried out. Both users felt comfortable while load bearing and could feel less muscle effort due to the self-locking characteristic of the device even during an abnormal gait (subject 2). During the swing phase there was not any issue and the user could bend the knee comfortably since the insole of rod 3 was not in contact with the ground.

6. Conclusions and future works

We have presented a new knee orthosis design encompassed within the group of SCKAFOs. It consists of a locking system that permits movement of the leg during the swing phase and locks the joint during the stance phase. There are three rods placed so that one of them allows fixation of the mechanism to the user's thigh, another connects the calf to the input of the mechanism so as to introduce power during the swing phase, and the third is anchored to the output of the mechanism, is responsible for any input of power through this output during the stance phase, and hence causes the mechanism to lock since power cannot be transmitted in that direction.

It should be noted that, unlike other orthosis designs proposed in the literature, this system is entirely mechanical. It therefore requires no electrical or electronic elements for its activation or deactivation. Also, it allows the knee to lock at any flexion angle during the stance phase. All this means that the characteristics of the proposed design can adapt to the gait of any user. Subjects with lower limb pathologies will benefit of the use of the SCKAFO presented on this paper. As has been proved in the trials carried out in this work, the mechanism self-locks in the presence of a force reaction and under different knee flexion angles. This will help users with muscle weaknesses such as trauma, multiple sclerosis, muscular dystrophy, unilateral leg paralysis, or paresis, as these subjects usually need orthosis that help them lock the knee during the gait cycle.

The orthosis developed in this work is a rigid device as it does not allow any knee flexion in order to absorb the impact of foot contact during the stance phase. Although it can self-lock at any knee flexion angle during the stance phase of gait, it lacks some force absorption before self-locking occurs. The subject however did not feel uncomfortable due to this limitation.

Finally, the device was also built and tested on two healthy subjects. In a qualitative way it has been demonstrated that the system self-locks while load bearing during the stance phase under different knee angles. For future works, lighter materials and considerations regarding the size of the device will be taken into account. Although in this work, a plastic support has been used in order to give some flexibility to the ankle joint, the authors will consider for future works the use of a klenzack spring, which will improve the rigidity of the ankle joint. As the purpose of the paper is to demonstrate the effectiveness of a completely mechanical orthosis that self-locks, we wanted to validate a new orthosis proposal. Due to the promising behavior of the device the device will also be tested on impaired users with lower limb injuries and further studies like energy consumption and muscle behavior will be analyzed.

References

[1] Rafiaei, M., Bahramizadeh, M., Arazpour, M., et al., 2015, "The Gait and Energy Efficiency of Stance Control Knee-Ankle-Foot Orthoses: A Literature Review," Prosthetics Orthotics Int., 40(2), pp. 202–214.

[2] Wang, W., Hou, Z., Tong, L., Zhang, F., Chen, Y., and Tan, M., 2014, "A Novel Leg Orthosis for Lower Limb Rehabilitation Robots of the Sitting/Lying Type," Mech. Mach. Theory, 74, pp. 337–353.
[3] Agrawal, K. S., 2005, "Design of Gravity Balancing Leg Orthosis Using Non-Zero Free Length Springs," Mech. Mach. Theory, 40(6), pp. 693–709.
[4] Arakelian, V., and Ghazaryan, S., 2008, "Improvement of Balancing Accuracy of Robotic Systems: Application to Leg Orthosis for Rehabilitation Devices," Mech. Mach. Theory, 43(5), pp. 565–575.
[5] Chen, G., Qi, P., Guo, Z., and Yu, H., 2006, "Mechanical Design and Evaluation of a Compact Portable Knee–Ankle–Foot Robot for Gait Rehabilitation," Mech. Mach. Theory, 103, pp. 51–64.
[6] Blaya, J. A., and Herr, H., 2004, "Adaptive Control of a Variable-Impedance Ankle–Foot Orthosis to Assist Drop-Foot Gait," IEEE Trans. Neural Syst. Rehabil. Eng., 12(1), pp. 24–31.
[7] Shorter, K. A., Kogler, G. F., Loth, E., Durfee, W. K., and Hsiao-Wecksler, E.T., 2011, "A Portable Powered Ankle–Foot Orthosis for Rehabilitation," J. Rehabil. Res. Dev., 48(4), pp. 459–472.
[8] Noel, M., Cantin, B., Lambert, S., Gosselin, C. M., and Bouyer, L. J., 2008, "An Electrohydraulic Actuated Ankle Foot Orthosis to Generate Force Fields and to Test Proprioceptive Reflexes During Human Walking," IEEE Trans. Neural Syst. Rehabil. Eng., 16(4), pp. 390–399.
[9] Horst, R. W., 2009, "A Bio-Robotic Leg Orthosis for Rehabilitation and Mobility Enhancement," International Conference of the IEEE Engineering in Medicine and Biology Society, pp. 5030–5033.
[10] Fleischer, G. H., 2008, "A Human–Exoskeleton Interface Utilizing Electromyography," IEEE Trans. Rob., 24(4), pp. 872–882.
[11] Tian, F., Hefzy, M. S., and Elahinia, M., 2015, "State of the Art Review of Knee–Ankle–Foot Orthoses," Ann. Biomed. Eng., 43(2), pp. 427–441.
[12] Shamaei, K., Napolitano, C., and Dollar, M., 2014, "Design and Functional Evaluation of a Quasi-Passive Compliant Stance Control Knee-Ankle-Foot Orthosis," IEEE Trans. Neural Syst. Rehabil. Eng., 22(2), pp. 258–268.
[13] Cullell, A., Moreno, J. C., Rocon, E., Forner-Cordero, A., and Pons, J. L., 2009, "Biologically Based Design of an Actuator System for a Knee-Ankle-Foot Orthoses," Mech. Mach. Theory, 44(4), pp. 860–872.
[14] Sawicki, G. S., and Ferris, D. P., 2009, "A Pneumatically Powered Knee–Ankle–Foot Orthosis With Myoelectric Activation and Inhibition," J. Neuroeng. Rehabil., (1), pp. 6–23.
[15] Yakimovich, T., Kofman, J., and Lemaire, E. D., 2009, "Engineering Design Review of Stance-Control Knee-Ankle-Foot Orthoses," J. Rehabil. Res Dev., 46(2), pp. 257–268.
[16] Salgado, D. R., and del Castillo, J. M., 2006, "Conditions for Self-Locking in Planetary Gear Trains," ASME J. Mech. Des., 129(9), pp. 960–968.
[17] Muller, H. W., 1982, Epicyclic Drive Trains, Analysis, Synthesis, and Applications, Wayne State University Press, Detroit, MI.
[18] Anderson, N. E., and Loewenthal, S. H., 1980, "Spur Gear System Efficiency at Part and Full Load," NASA, , Technical Paper No. 1622, Technical Report No. 79-46. 580
[19] Diab, Y., Ville, F., and Velex, P., 2006, "Prediction of Power Losses Due to Tooth Friction in Gears," Tribol. Trans., 49(), pp. 266–276.
[20] AGMA, 1988, "Design Manual for Enclosed Epicyclic Metric Module Gear Drives," American Gear Manufacturers Association, , Standard No. 6123- A88.
[21] del Castillo, J. M., 2002, "The Analytical Expression of the Efficiency of Planetary Gear Trains," Mech. Mach. Theory, 37(2), pp. 197–214.
[22] Li, S., 2012, "Contact Stress and Root Stress Analyses of Thin-Rimmed Spur Gears With Inclined Webs," ASME J. Mech. Des., 134(), .
[23] Hwang, S. C., Lee, J. H., Lee, D. H., Hana, S. H., and Lee, K. H., 2013, "Contact Stress Analysis for a Pair of Mating Gears," Math. Comput. Modell., 57(1–2), pp. 40–49.
[24] Patil, S., Karuppanan, S., Atanasovska, I., and Wahab, A. A., 2014, "Frictional Tooth Contact Analysis Along Line of Action of a Spur Gear Using Finite Element Method," Proc. Mater. Sci., 5, pp. 1801–1809.

Mech. Sci., 9, 359–371, 2018
https://doi.org/10.5194/ms-9-359-2018

Mechanical Sciences
Open Access

A new manual wheelchair propulsion system with self-locking capability on ramps

Gaspar Rodríguez Jiménez[1], David Rodríguez Salgado[1], Francisco Javier Alonso[1], and José María del Castillo[2]

[1]Department of Mechanical Engineering, University of Extremadura, Badajoz, 06006, Spain
[2]Department of Material Science and Transportation Engineering, University of Seville, Badajoz, 41092, Spain

Correspondence: Gaspar Rodríguez Jiménez (gaspar.rodriguez.jimenez@gmail.com)

Received: 15 February 2018 – Revised: 3 October 2018 – Accepted: 23 October 2018 – Published: 8 November 2018

Abstract. A wheelchair user faces many difficulties in their everyday attempts to use ramps, especially those of some length. The present work describes the design and build of a propulsion system for manual wheelchairs for use in ascending or descending long ramps. The design is characterized by a self-locking mechanism that activates automatically to brake the chair when the user stops pushing. The system consists of a planetary transmission with a self-locking capacity coupled to a push rim with which the user moves the system. Different transmission ratios are proposed, adapted to the slope and to the user's physical capacity (measured as the power the user can apply over ample time periods). The design is shown to be viable in terms of resistance, and approximate dimensions are established for the height and width of the propulsion system. Also, a prototype was built in order to test the self-locking system on ramps.

1 Introduction

There are several types of manual wheelchairs, among which there stands out the basic manual push rim propelled models (Vanlandewijck et al., 2001; van der Woude et al., 2001). These account for around 90 % of the chairs existing on the market. They are the most commonly used due to their low cost, their excellent handling capacity, and ease of transportation since they can be folded (van der Woude et al., 2006). Another type that stands out is the crank-propelled wheelchair. This uses the same type of propulsion as bicycles and its most efficient configuration is that of handcycling, where propulsion is powered using the hands (Arnet et al., 2013). Another type is the lever-propelled wheelchair which uses a lever fixed directly to the rim, allowing the user to adopt a more ergonomic position and being more efficient than the crank-propelled wheelchair (van der Woude et al., 2001). The last type of chair with manual propulsion is the geared manual wheelchair which functions with mechanical geared wheels (Flemmer and Flemmer, 2016).

Ramps are a major problem for users' everyday lives. This is especially so for the long ramps that they encounter in cities, since activities that require changes of inertia need more upper limb strength than those needed to maintain speed on the flat (Sonenblum et al., 2012).

There are some devices in the literature that allow the users to use geared transmissions for manual wheelchairs propulsion but not many of them complement the propulsion with a locking mechanism when ascending or descending a ramp. Magicwheels is a commercial brand (Meginniss and SanFrancisco, 2006) that uses a transmission based on a hypocycloidal which has two modes. In the standard mode the hand rim is connected directly to the wheel and the system behaves like a normal pushrim propelled wheelchair. If the user pushes a shift on the hub, the gear turns into a transmission providing a gear ratio lower than 1 : 1 which helps wheelchair users to ascend a ramp easily. It also has a hill holding mechanism which prevents the wheelchair from rolling backwards. This hill holder mechanism includes one way roller assemblies in order to rotate in one direction but not the other. Thus, the locking of the mechanism is achieved through friction preventing the gear assembly from moving backwards. The device is mounted on a wheel, and the user would replace its own wheel in order to use this propulsion system.

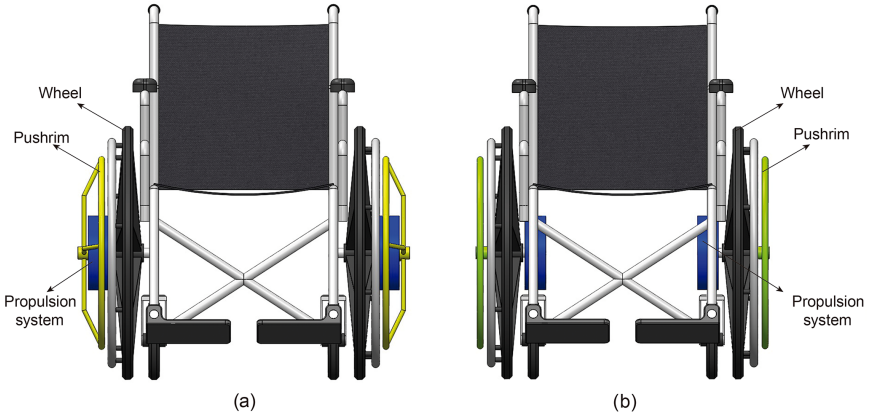

Figure 1. Different arrangements of the propulsion system: **(a)** between the wheel and the power input element; **(b)** under the seat.

In this work, a propulsion system is proposed whose main component is a wheel-locking system based on a self-locking planetary gear train (PGT) that can be attached to any manual wheelchair. Since the self-locking PGT is a mechanism in which the input and output are coaxial, it can be feasibly coupled to any wheelchair. The input of the mechanism is connected to push rims through which the user can apply power to the propulsion system, and this then transmits the movement to the chair. However, if the power is transmitted from the wheels themselves (which are connected to the output of the mechanism), the system does not allow movement due to its self-locking nature. The system is ideal for long ramps, where its use helps reduce the effort needed over a long period of time, preventing the user becoming fatigued, and allowing them to ascend or descend a long slope.

In the following sections, we shall describe firstly the possible arrangements and transmission ratios of the propulsion system that are required to climb ramps of different slopes, based on different power inputs. Then, a proposed design of the self-locking system and details of the propulsion system will be described. Finally, a functional and qualitative evaluation of the prototype will be tested on a ramp.

2 Possible layout arrangements of the propulsion system

The main element of the propulsion is a PGT. This is a coaxial transmission with a single degree of freedom, so that it has to have a fixed member to operate correctly but can be attached to any wheelchair. In particular, the system can be implemented directly between the wheel and the power transmission element (the push rim) as shown in Fig. 1a, or under the chair with a different configuration as shown in Fig. 1b. This latter is the option chosen for the present work.

The need to have a mechanism with one degree of freedom requires one of the elements of the system to be established as a fixed member ($\omega = 0$). For this reason, the housing containing the propulsion system is fixed to the chassis of the wheelchair. To explain the behaviour of the propulsion system, Fig. 2 shows the two situations that can occur when a manual wheelchair user is on a ramp. In Fig. 2a, the power input is from the push rim. In this case, the mechanism is capable of transmitting power and thus moving the wheel. However, when the power input is through the wheel, i.e., when the user is not moving the push rim, the configuration of the system prevents power being transmitted to the output member, and the movement of the chair is locked, as is shown in Fig. 2b.

Thus, with this system, the user can resume propelling the chair at will without needing to activate or deactivate any wheel locking mechanism. Also, the effects of inertia when the user is on a ramp do not have to be overcome since the mechanism locks when power input is through the wheels. The same is the case when motion is resumed, i.e., it is not necessary to overcome the effects of inertia when power is input through the push rim.

3 Analysis of the kinematics of the proposed propulsion system

There are various factors that influence the manual propulsion of a wheelchair, such as the type of surface on which the chair is being propelled (Koontz et al., 2005), the individual's mass (Sprigle and Huang, 2015), and the slope of the terrain (Choi et al., 2015). Upper trunk activity increases as the slope becomes steeper, but the use of any reduction mechanism that increases the torque applied to the axis of the chair decreases the performance of certain muscle groups of the user's upper trunk (Howarth et al., 2010). Figure 3 shows the forces on the propulsion wheel when the user is on a slope, assuming that the chair moves with constant speed.

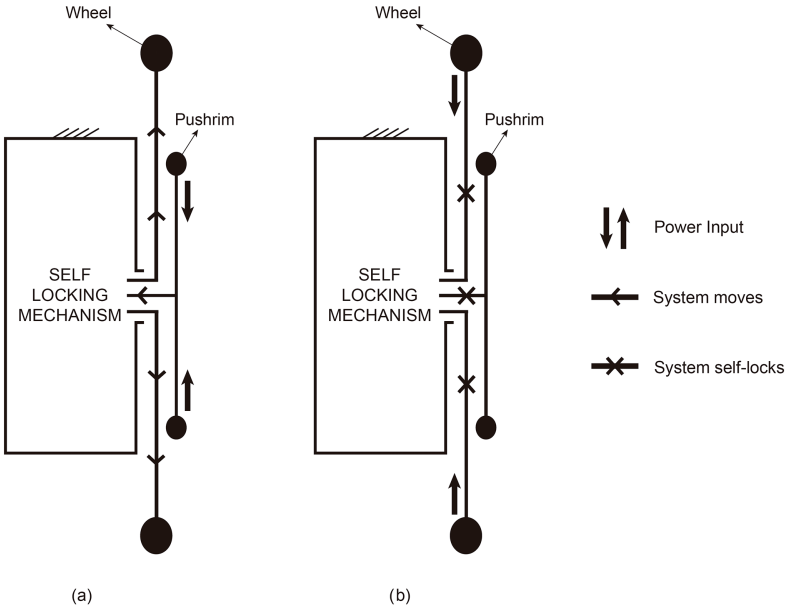

Figure 2. Action of the propulsion system when: **(a)** power is input through the push rim (the propulsion system functions); **(b)** power is input through the wheels (the propulsion system has self-locked).

In this figure F_{drag} is the rolling resistance force, α is the slope of the ramp, $F_{\text{t}(\alpha>0)}$ is the tangential force the subject needs to apply to move the chair when $\alpha > 0$, and ϕ is the angle with the horizontal formed by the radius to the point of application of the tangential force. This force causes the propulsion torque M_{c}^{α} at the centre of the wheel. It can be seen that the total force is $F = \sqrt{F_{\text{t}(\alpha>0)}^2 + F_{\text{r}}^2}$ with the purely tangential force $F_{\text{t}(\alpha>0)}$ being responsible for the forward movement of the wheelchair (Boninger et al., 1997, 2002; Chow et al., 2009; Dallmeijer et al., 1994; De Groot et al., 2002; Kwarciak et al., 2009; Lin et al., 2009; Robertson et al., 1996; Veeger et al., 1991; van der Woude et al., 1988), and F_{r} being the normal component which, although it does not move the chair, plays a part in the friction between the hand and the push rim.

We make the following simplifying assumptions in this work: the analysis is done in two dimensions (van der Woude et al., 1988); the speed of ascent ($v_{\text{slope}} = \text{cte}$) (Arnet et al., 2013; Chow et al., 2009; Veeger et al., 1991; Van Der Woude et al., 2003); the inertia of the wheel (Richter et al., 2007; van der Woude et al., 1988) and the aerodynamic resistance (Van Der Woude et al., 2003, 1988) are neglected; and the forces the user applies to each wheel are symmetrical (Arnet et al., 2013). Then:

$$F_{\text{t}(\alpha>0)} = F_{\text{p}} + F_{\text{drag}} \tag{1}$$

Given $F_{\text{t}(\alpha>0)}$ one can determine the torque M_{c}^{α} needed to move the chair up a ramp. Taking a total mass (chair + user) of $m = 100\,\text{kg}$ and a coefficient of rolling resistance $\rho = 0.015$ in accordance with the results reported in de Groot et al. (2006) and Richter et al. (2007), one has:

$$\begin{aligned} M_{\text{c}}^{\alpha} &= F_{\text{t}(\alpha>0)} \cdot r_{\text{p}} = \left(F_{\text{drag}} + F_{\text{p}}\right) \cdot r_{\text{p}} \\ &= (\rho\, \text{mgcos}\,\alpha + \text{mgsin}\,\alpha) \cdot r_{\text{p}} \end{aligned} \tag{2}$$

Where r_{p} is the radius of the pushrim, which we take 0.225 m. The power input PI applied directly to the pushrim is given by:

$$\text{PI} = M_{\text{c}}^{\alpha} \cdot \omega_{\text{slope}}(W) \tag{3}$$

Where $\omega_{\text{slope}} = v_{\text{slope}}/r_{\text{w}}$ is the angular velocity in rad s^{-1} of the wheels on the slope, with r_{w} being the radius of the wheel which we take $r_{\text{w}} = 0.27\,\text{m}$.

In this work, we took an individual's physical condition to be the power that they can input at a constant rate for an ample period of time. In Salgado and Castillo (2007), it is explained that for a planetary propulsion system to be self-locking, it must be designed in such a way that the mechanism is one of reduction. In this sense, the propulsion system's transmission ratio (R_{t}) is obtained as a function of PI and the slope to ascend. To calculate v_{slope}, we set $v_l = 1.2\,\text{m s}^{-1}$ which is the speed that the chair would have on the flat without using the propulsion system, and then $v_{\text{slope}} = R_{\text{t}} v_l$.

Figure 4 shows power input to the push rim for different values of v_{slope} (with R_{t} being 1/12, 1/6, 1/4, 1/3 and 5/12) for $v_l = 1.2\,\text{m s}^{-1}$. For this study, we considered that ramp slopes of less than 4 % are too little, and greater than 10 % are too steep, for the propulsion system to be used. The suitable values are represented by a shaded area in Fig. 4 and, while it is not a criterion for the choice of the propulsion system, it

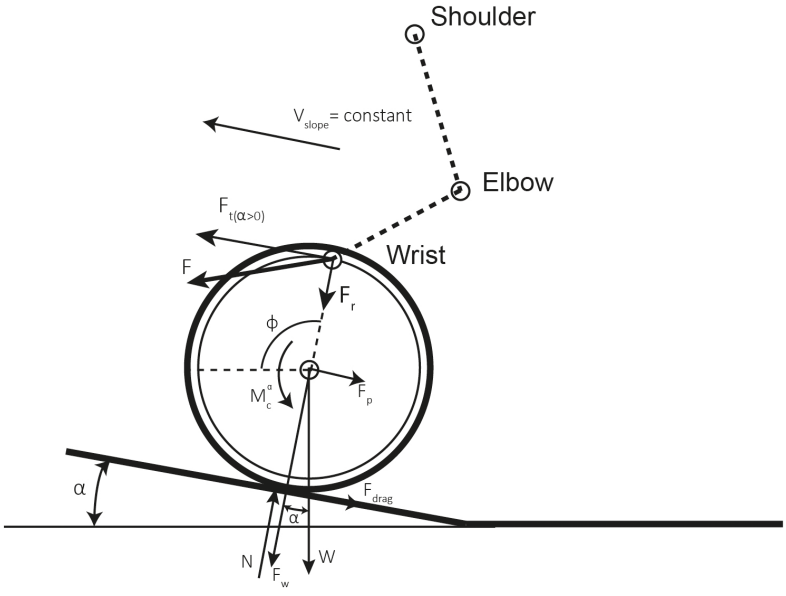

Figure 3. The forces and torques on the push rim of the wheelchair when climbing a slope at constant speed.

does establish an approximation of the minimum and maximum ramps that a user can take on. The figure represents by way of example a user whose physical capacity allows them to input PI = 50 W at the push rim. Depending on the slope to ascend, one obtains the corresponding values of R_t represented by the points (P_1, P_2, P_3, P_4). With the same PI, the user is able to climb ramps ranging from 4.7% at a speed of $v_{slope} = 0.5\,m\,s^{-1}$ to 13.7 % at a speed of $v_{slope} = 0.2\,m\,s^{-1}$. This graphic thus makes it possible to clearly see the values of R_t the user will need to climb certain ramps depending on the PI they are capable of.

The behaviour of the propulsion system was verified by a simulation in which a user wishes to climb a ramp of approximately 5 % slope and is capable of inputting a power PI = 50 W for a long period of time. Taking $v_l = 1.2\,m\,s^{-1}$ as in Fig. 4, one can see that these data correspond approximately to the point P_1, with $R_t = 5/12$, i.e., $v_{slope} = 0.5\,m\,s^{-1}$. Figure 5 shows the user performing a complete push cycle while climbing a ramp. When the user stops inputting power, the system locks (Fig. 5b). When, at any time, the user wishes to resume the ascent they can do so by simply applying power to the push rim, avoiding having to overcome the force of inertia.

Now that one knows the transmission ratios that are best adapted to each user depending on their physical condition and the slope that they want to ascend, in the following section we shall explain the design of the self-locking propulsion system.

4 Design of the self-locking propulsion system

For a PGT to be self-locking, it must satisfy a series of design conditions which mean that only a small set of construction solutions are possible (Salgado and Castillo, 2007). In this section, we shall determine a solution for the self-locking system proposed in Fig. 2.

For simplicity of construction, we shall analyse the two 4-member self-locking PGT solutions since these are the ones with the fewest possible members (Fig. 6). For the design proposed in the present work, we chose the solution of Fig. 6a because it has gear pairs that are external (gear/gear) rather than internal (gear/ring gear). For this construction solution to be self-locking, the following expression must be satisfied (Salgado and Castillo, 2007):

$$\eta_{14}\eta_{24} < \frac{Z_{24}}{Z_{14}} < \frac{1}{\eta_{14}\eta_{24}} \tag{4}$$

where η_{ij} is the ordinary efficiencies of the circuits of the PGT. The ordinary efficiency is the efficiency of the gear pair if the arm linked to the planet were fixed. By means of this efficiency, one introduces into the overall efficiency calculation of the gear train the friction losses that take place in each gear pair. Although the value of the ordinary efficiency in each gear pair depends on the number of teeth of its gears, on the operating conditions (applied torque, speed, lubricant type and method, temperature), and on geometric factors such as the approach portion and the recess portion and on tooth surface roughness (Anderson and Loewenthal, 1980; Diab et al., 2006; Müller, 1982; Xu and Kahraman, 2005), for the analysis of the self-locking conditions; it is sufficient to consider a value of the ordinary efficiencies slightly less than unity

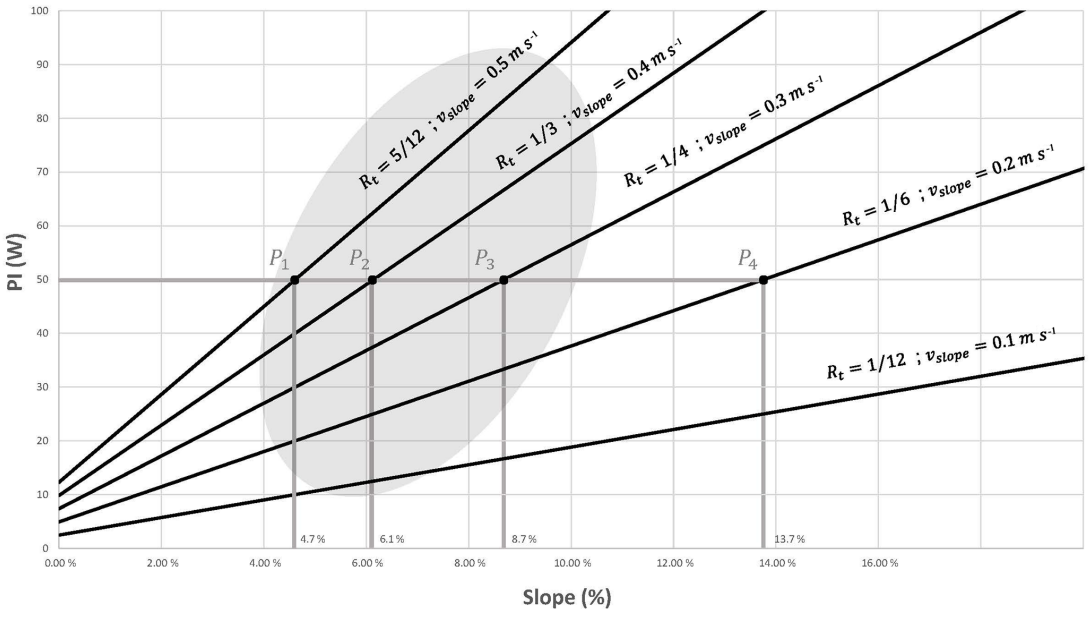

Figure 4. Diagram of the transmission ratios R_t and speed of climb for a given $v_l = 12\,\mathrm{m\,s^{-1}}$ as functions of the slope to ascend and the power PI that the user inputs to the chair.

(Salgado and Castillo, 2007). In Eq. (4) Z_{ij} is the tooth ratio of the gear pair formed by the linking members i and j. In particular, Z_{ij} is defined as $Z_{ij} = Z_i/Z_j$. For the definition of the tooth ratios to satisfy the Willis equations, Z_{ij} must be positive if the gear is external (meshing gear–gear) and negative if it is internal (meshing ring gear–gear). For the train of Fig. 6a, one would have to take $Z_{14} > 0$ and $Z_{24} > 0$.

The two construction solutions for a 4-member self-locking PGT only allow power flow with input through the arm (Member 3) and output through the sun (Member 1), as shown in Fig. 6, where the power flow is in the direction marked by the arrow. The transmission ratio of the four-member PGT with input through the arm is (Salgado and Castillo, 2007):

$$r = \frac{Z_{14} - Z_{24}}{Z_{14}} \tag{5}$$

For the design of the wheelchair locking system based on PGTs, we have considered the constraints on this type of transmission. These constraints can be grouped into two categories – one involving gear size and geometry, and the other the PGT meshing requirements, as will be detailed in the following two subsections.

4.1 Constraints involving gear size and geometry

The first constraint is a practical limitation of the range for the acceptable face width b. This constraint is as follows:

$$9m < b < 14m \tag{6}$$

Where m is the module of the gears. All of the kinematic and dynamic parameters of the transmission depend on the values of the tooth ratios Z_{ij}. In theory, the tooth ratios can take any value, but in practice, they are limited mainly for technical reasons because of the difficulty in assembling gears outside of a certain range of tooth ratios. In this work, the tooth ratio for the design of mechanical spindle speeders are quite close to the recommendations of Müller (1982) and the American Gear Manufacturers Association (AGMA) norm (American Gear Manufacturers Association, 1988), and are:

$$0.2 < Z_{ij} < 5 \tag{7}$$

$$-7 < Z_{ij} < -2.2 \tag{8}$$

with the constraint given by Eq. (7) being for external gears and that by Eq. (8) for internal gears. It is important to note that these constraints are valid for designs with different numbers of planets (N_p) (Müller, 1982).

Another constraint that will be imposed on the design of 4-PGT with double planets, as the self-locking PGT implemented in the locking system design, is that the ratio of the diameters of the gears constituting a double planet is:

$$\frac{1}{3} < \frac{d_4}{d_{4'}} < 3 \tag{9}$$

where d_4 and $d_{4'}$ are the pitch diameters of the gears than constitutes the planet gear that meshes with members 1 and 2 (see Fig. 6).

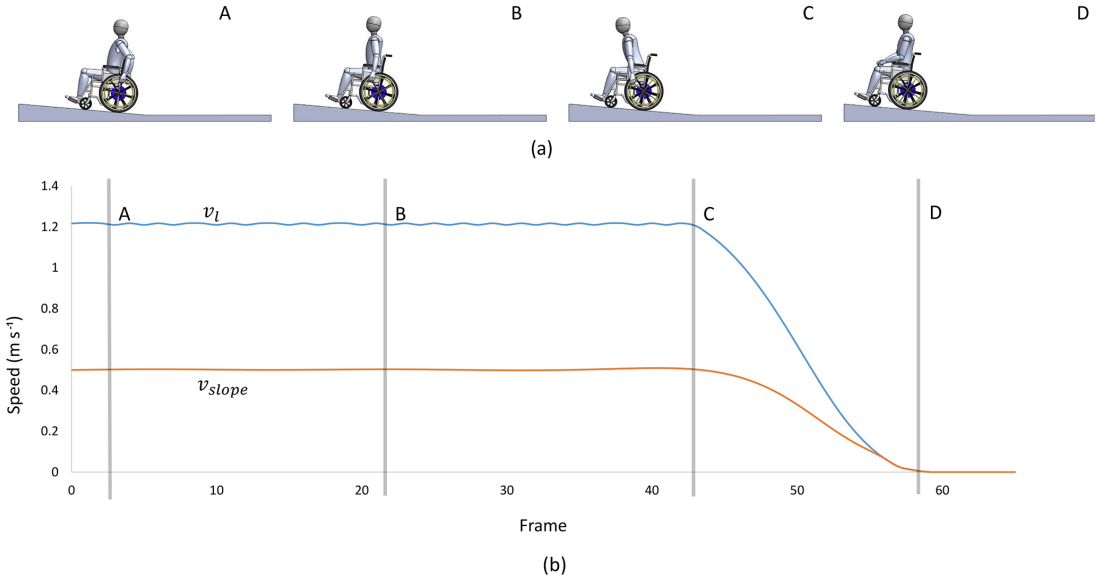

Figure 5. Simulation of the ascent of an approximately 5 % slope with velocity $v_l = 1.2\,\mathrm{m\,s^{-1}}$ and $R_t = 5/12$. **(a)** The stages of a push cycle in which step A is the start, B is halfway through the push, C is the end of the push cycle, and D is when the user stops inputting power while still situated on the ramp; **(b)** the corresponding speeds v_l and v_{slope}.

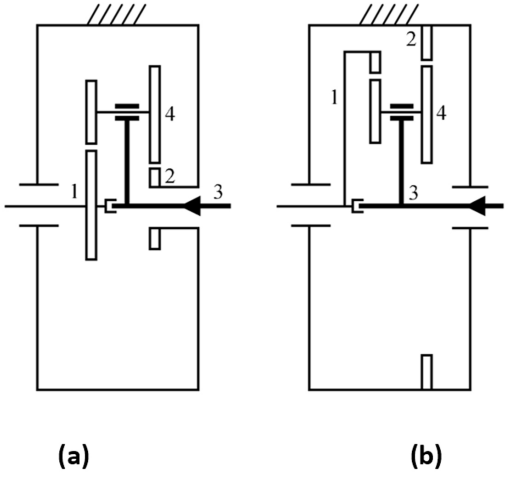

Figure 6. Construction solutions for four-member planetary gear trains. **(a)** External gears. **(b)** Internal gears.

4.2 Planetary gear train meshing requirements

The meshing requirements are given by the AGMA norm (American Gear Manufacturers Association, 1988). For planetary systems with double planets must, either of which, factorise with the number of planets in the sense of Eq. (10) below (see AGMA norm; American Gear Manufacturers Association, 1988):

$$\frac{Z_2 P_2 \pm Z_1 P_1}{N_p} = \text{an integer} \tag{10}$$

where P_1 and P_2 are the numerator and denominator of the irreducible fraction equivalent to the fraction $Z_{4'}/Z_4$; where $Z_{4'}$ is the number of teeth of the planet gear that meshes with member 1 and Z_4 is the number of teeth of the planet gear that meshes with member 2 (see Fig. 6):

$$\frac{Z_{4'}}{Z_4} = \frac{P_1}{P_2} \tag{11}$$

It can be verified that to satisfy the above requirements, and given that the 4-member PGT with arm input is a reduction transmission, the maximum transmission ratio (minimum reduction) that can be achieved so that a self-locking train is obtained, i.e., so that the constraints of Eqs. (4)–(11) are satisfied, is the one that has $R_t = 1/12$. Of the possible transmission ratios for a self-locking PGT, we chose this maximum.

As a specific design proposal to achieve $R_t = 1/12$, we propose the following teeth numbers for the self-locking PGT: $Z_1 = 48$, $Z_2 = 44$, $Z_4 = 20$ and $Z_{4'} = 20$.

As mentioned above, and as can be checked in Fig. 4, the logical R_t values go from 5/12 to 1/12. Therefore, only in one case is the propulsion system a self-locking PGT. For the rest of the PI and slope values, a self-locking PGT + multiplier combination is necessary. In this work, we propose a PGT as multiplier stage since the speed is multiplied in a single step.

The self-locking PGT design with the planet member consisting of four gears ($N_p = 4$) is shown in Fig. 7a, and Fig. 7b is a schematic diagram of the complete propulsion system (self-locking PGT + multiplier PGT). The self-locking PGT is common to any design of the propulsion system. The mem-

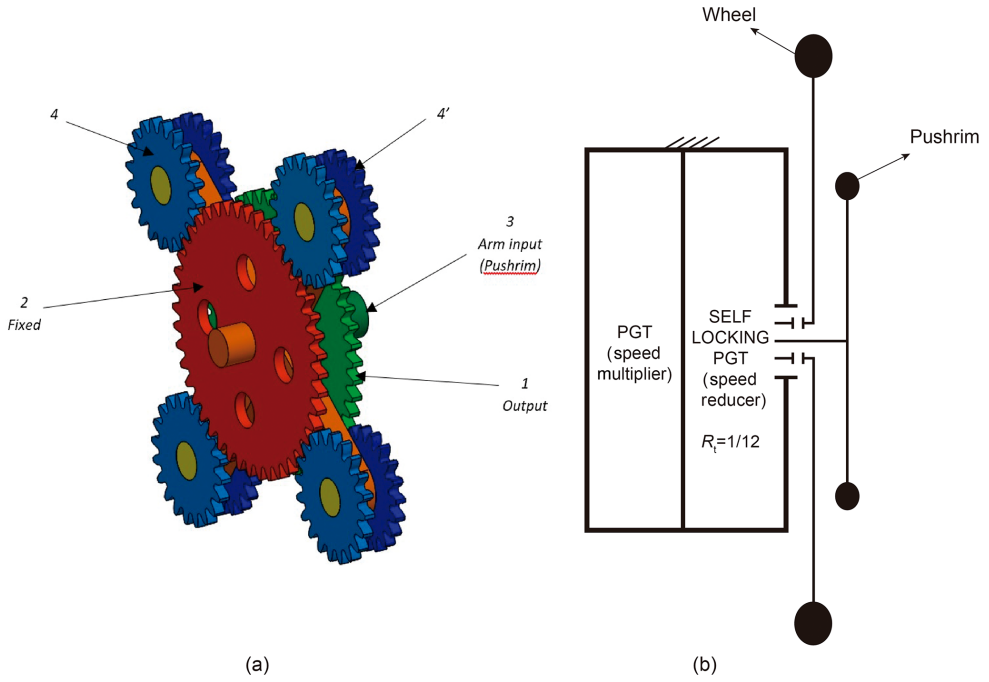

Figure 7. **(a)** Design of the self-locking Planetary Gear Train with $R_t = 1/12$. **(b)** Scheme of the complete propulsion system.

ber that varies depending on the needs of the user is the multiplier stage.

4.3 Force and stress analysis

As an example, we use an intermediate transmission ratio $R_t = 5/12$, which is the result of combining a self-locking PGT with $R_t = 5/12$ and a multiplier PGT with $R_t = 5$. The objective is to evaluate whether the propulsion system is small in size. To perform the calculations, two phases must be distinguished: when the system is locked, and when PI is input through the pushrim.

In the locking phase of the propulsion system, the value of R_t of the system is irrelevant since the stresses produced in the system depend solely on the slope and the chair-plus-user mass. For the calculations in this phase, one must decide on the value of the slope. We shall take a slope of 10 %. Since the system is locked, $F_{drag} = 0$ because it is not necessary to overcome any forces of friction. Thus, considering $m =$ 100 kg, the only force that the system supports is that of the weight, F_p:

$$F_{t(\alpha>0)} = F_p + F_{drag} = mg\sin\alpha + 0 = 97.6\,N \quad (12)$$

The radius of the Wheel, r_w is 270 mm. If no reduction system is used, the torque produced on the wheel's axis during this locking phase on a slope of 10 % will be:

$$M_c^{\alpha} = F_p r_w = 26.35\,\text{Nm} \quad (13)$$

This torque is distributed symmetrically through the two drive wheels. Hence, each locking system receives a torque of $M_c^{\alpha} = 13.17$ Nm. Each drive wheel is connected to the self-locking PGT's output gear (Gear 1) which will receive the full torque, and trigger the locking. Using the values given in Table 1 for the dimensions of the elements conforming the propulsion system, the tangential force produced by $M_c^{\alpha} = 26.35$ Nm on the cogs of Gear 1 will be $F_{t(\alpha>0)} =$ 233.2 N. Since they belong to the same member, planets 4′ and 4 distribute the torque produced by the locking symmetrically, and this will be that given by the tangential force exerted by the cogs of Gear 1. Figure 8 shows a method for calculating the resistance of the mechanism. This is the method used in Hwang et al. (2013), Li (2012), Moreira et al. (2016) and Patil et al. (2014) in which the resistance of the cog is calculated from the tangential force $F_{t(\alpha>0)}$ caused by the torque produced at the centre of the gear's pitch radius.

When power is input through the push rim, the equations proposed in Del Castillo (2002) are used to calculate the torques and angular velocities of the components of the propulsion system (self-locking PGT + multiplier PGT) with power input to the self-locking PGT through the arm. These calculations were done using software developed in Matlab based on the aforementioned equations. Table 1 gives the size and dynamic characteristics of each member of the mechanism when a torque M_c^{α} is input through the push rim. For the dynamics calculations, we considered the values of R_t represented in Fig. 4.

The increase in the torques produced in the self-locking PGT elements is due to the power recirculation that occurs in this type of self-locking PGT (Del Castillo, 2002). Thus,

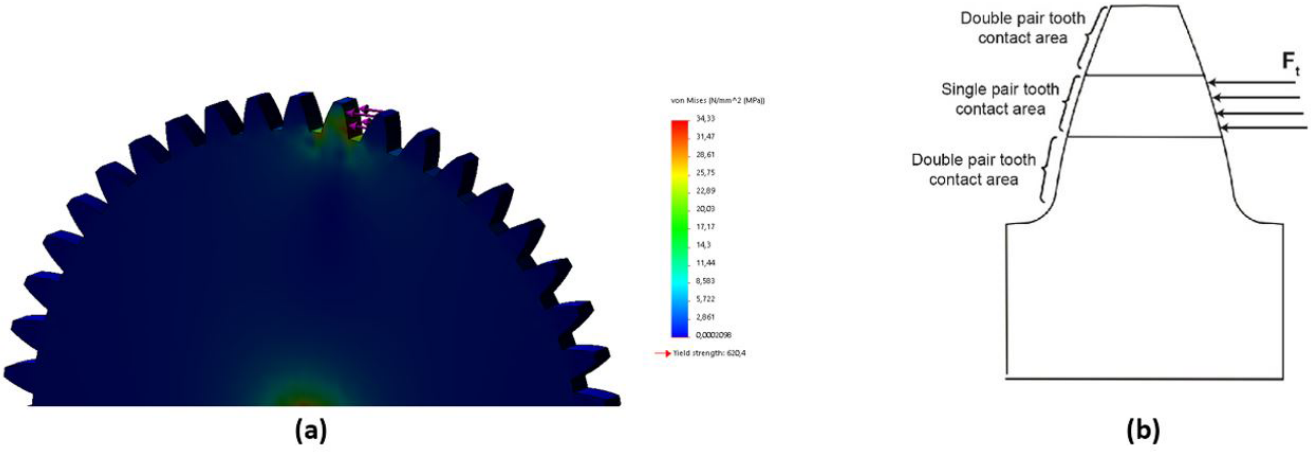

Figure 8. **(a)** Stresses produced by the tangential forces applied to the cog during the blocking phase. **(b)** Areas in which the different contacts occur, and the application of the tangential force F_t^{α} produced by the contact in the least favourable area.

Table 1. Size characteristics of the gears conforming the propulsion system, and the contact ratios between elements in contact and the dynamic loads on each element when M_c^{α} is input through the pushrim.

System	Member	Teeth	Pitch Diameter (mm)	Thickness (mm)	Module (mm)	Contact Ratio (xN_p)	Torque (Nm)	Angular speed (rpm)
	Arm	–	–				M_c^{α}	ω_l
Self-locking PGT ($R_t = 1/12$)	1	48	113	5	2.35	1.61 (×4)	$5.79M_c^{\alpha}$	$1/12\omega_l$
	$4'$	20	47				$2.29M_c^{\alpha}$	$3.2\omega_l$
	2	44	110		2.5	1.64 (×4)	$4.79M_c^{\alpha}$	0
	4	20	50				$2.29M_c^{\alpha}$	$3.2\omega_l$
Multiplier ($R_t = 5$)	Ring	120	180	5	1.5	> 3 (×3)	$4.67M_c^{\alpha}$	0
	Planet	45	67.5			1.695 (×3)	$1.72M_c^{\alpha}$	$1.66/12\omega_l$
	Sun	30	45				$1.12M_c^{\alpha}$	$5/12\omega_l$
Multiplier ($R_t = 4$)	Ring	90	180	5	2	> 3 (×3)	$4.39M_c^{\alpha}$	0
	Planet	30	60			1.654 (×3)	$1.43M_c^{\alpha}$	$1/6\omega_l$
	Sun	30	60				$1.40M_c^{\alpha}$	$1/3\omega_l$
Multiplier ($R_t = 3$)	Ring	80	160	5	2	> 3 (×4)	$3.91M_c^{\alpha}$	0
	Planet	20	40			1.635 (×4)	$0.96M_c^{\alpha}$	$1/4\omega_l$
	Sun	40	80				$1.88M_c^{\alpha}$	$1/4\omega_l$
	Arm	–	–		–		$2.77M_c^{\alpha}$	$1/6\omega_l$
Multiplier ($R_t = 2$)	2	60	99.6	5	1.66	1.719 (×3)	$5.79M_c^{\alpha}$	$1/12\omega_l$
	$4'$	30	49.8				$2.95M_c^{\alpha}$	$1/3\omega_l$
	1	30	75		2.5	1.654 (×3)	$2.77M_c^{\alpha}$	0
	4	30	75				$2.95M_c^{\alpha}$	$1/3\omega_l$

unlike in the locking phase of the system when the maximum torque supported by the self-locking PGT is limited by the size of the gears and the weight of the user, in this phase the limiting variable is the torque that is input onto the push rim where the greatest stresses arise.

As an example, we present a calculation of the stresses that arise on the cogs of the PGT's gears when a user is able to input a power of approximately 70 W, and wishes to climb a 7 % ramp. According to Fig. 4, the transmission ratio that is best suited to the needs of this case is $R_t = 5/12$. The speed of ascent, $v_{slope} = 0.5\,m\,s^{-1}$ is the consequence of inputting approximately $M_c^{\alpha} = 19\,Nm$ at $\omega_l = 4.44\,rad\,s^{-1}$, which means that 9.5 Nm is applied to each push rim. As one observes in Table 1, taking into account the dimensions of the components of both the self-locking and the multiplier stages, the component which supports the greatest stress is Planet $4'$ of the self-locking PGT. The results of the dynamic simulation with this force applied to the cog as in Fig. 8 are shown in Fig. 9.

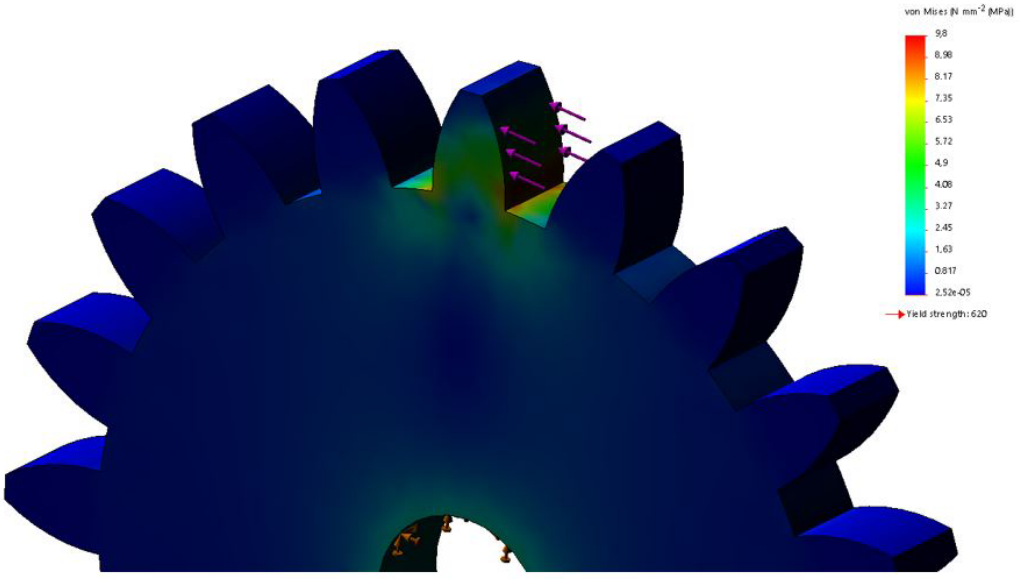

Figure 9. Stresses produced by the tangential forces applied to the cog when the user inputs power through the push rim: the dynamic loads on Member 4′ (the least favourable).

Table 2. Characteristics of the elements conforming the proposed propulsion system with $R_t = 5/12$.

Member	Material (Density)	Mass	Total Member mass (g)	Thickness (mm)	Diameter (mm)
Arm	Rigid PVC	111.86	628.14	10	–
Z2	Alloyed cast steel	311.54	311.54	5	110
Z4	Alloyed cast steel	63.16	252.64	5	50
Z4′	Alloyed cast steel	55.11	220.44	5	47
Z1	Alloyed cast steel	355.33	355.33	5	113
Ring	Alloyed cast steel	474.91	474.91	5	200
Sun	Alloyed cast steel	277.76	277.76	5	100
Planet	Alloyed cast steel	65.87	197.61	5	50
Planets carrier	Rigid PVC	173.4	173.4	5	–
		Total	2891.77	30	202.5 (dedendum diameter)

The cogs of Member 4′ can withstand the effects produced even in situations of steep slopes. This method has therefore allowed us to define the thicknesses and diameters of all the gears, and hence we can also define the approximate dimensions of the complete propulsion system.

With the stresses that arise in the elements of the propulsion system known, and its viability in terms of resistance confirmed, we can now approximate the overall dimensions of the system, as is illustrated in Fig. 10a for $R_t = 5/12$. An exploded view of the mechanism is included in Fig. 10b.

Table 2 lists the specifications of each element of the transmission for $R_t = 5/12$. A relationship is established between the width and the height of the casing enclosing the transmission in order to have an approximation of the system's viability in terms of its dimensions.

5 Functional and qualitative evaluation

In this work a prototype of the propulsion system has been tested in order to validate the reliability and the behaviour of the self-locking system in manual wheelchairs. The gears that formed the self-locking PGT and the multiplier stage were made of alloy steel. A ball bearing was used in gear 1 with 12 mm of diameter, the rest of the bearings of the prototype were needle bearings with 10 mm diameter each. The mounting of the prototype was as follows: gear 2 and the first part of the housing were joined together with screws which prevented gear 2 from moving. Planet gears 4 and 4′, the planet carrier and the input arm were mounted together. In this prototype a speed multiplier with a speed ratio of 5 : 1 was mounted at the output of gear 1. The sun element of the speed multiplier (output of the transmission) was connected to the wheel of the wheelchair. The second part of

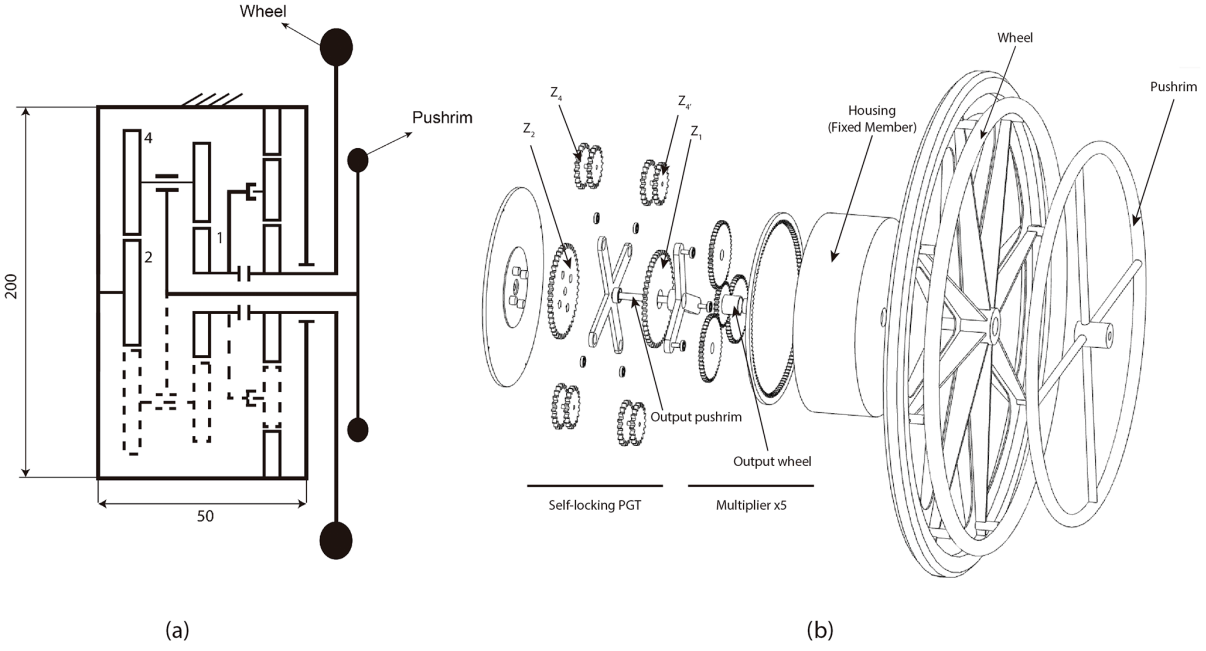

Figure 10. **(a)** Diagram of the final transmission with the approximate values in mm of the width and height of the casing enclosing it, **(b)** Exploded view of the propulsion mechanism using a stage multiplier $\times 5$.

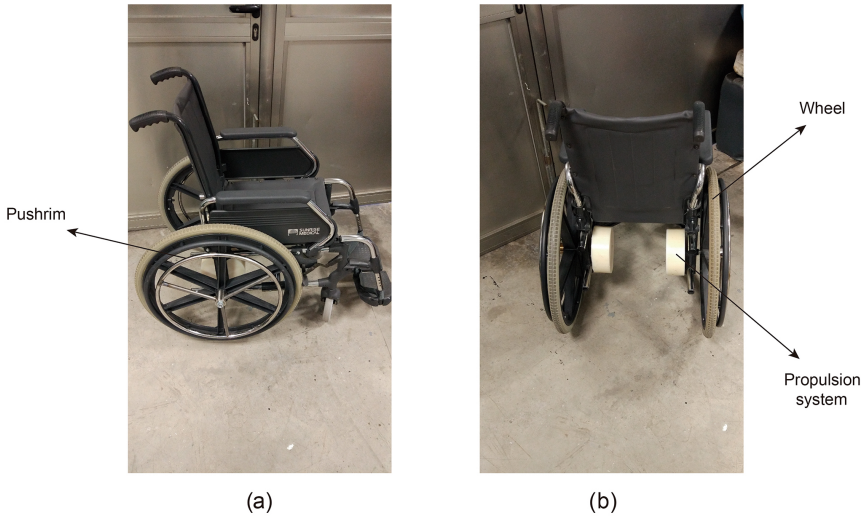

Figure 11. **(a)** Side view of the manual wheelchair with the propulsion system. **(b)** Rear view.

the housing encapsulated the transmission, thus forming an assembly which was subsequently joined to the chassis of the wheelchair using screws, leaving the housing as the fixed element of the transmission. An external pushrim was installed and connected to the input arm with the purpose of introducing power to the propulsion system. As mentioned in Fig. 1 there were two possible arrangements for the transmission, and the decision was taken to mount the prototype underneath the seat as can be seen in Fig. 11b which shows a rear view of the wheelchair. This configuration does not increase the width of the whole system. Once the prototype was mounted, the transmission had a $R_t = 5/12$.

The trials were conducted on a healthy subject with a height of 1.80 m and a mass of 80 kg. The ramp used for the trials was located at the main entry of a residential area, it had a 10 % slope and a length of 15 m. The first trial consisted of analysing the self-locking characteristic of the prototype. The subject was told to remain stationary and not to move the external pushrim. While the subject was on the slope in an uphill direction the power input was transferred from the

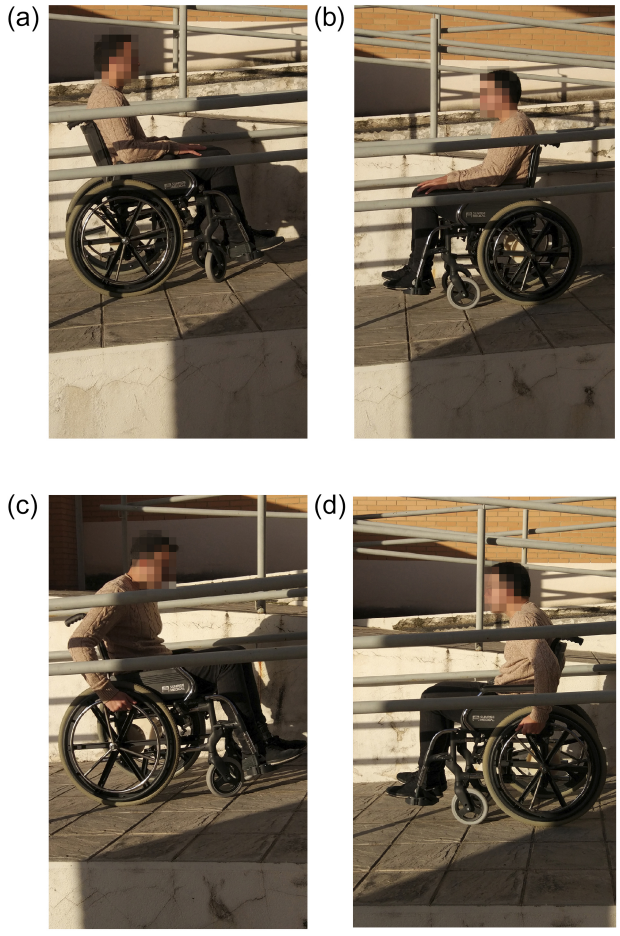

Figure 12. **(a, b)** Different views of the propulsion system without power input (system self-locks) during both ascending **(a)** and descending trials **(b)**. **(c, d)** Different views of the propulsion system with power input through the external rim (system moves) during both ascending **(c)** and descending trials **(d)**.

wheel to the output of the self-locking PGT (gear 1), provoking the locking of the system and preventing the subject from rolling backwards. In the same way, when the subject was in a downhill direction, the prototype also self-locked. The subject was comfortable and did not feel any risk of rolling backwards or forwards while the prototype was locked. As can be seen in Fig. 12, panel (a) shows the user on an uphill ramp and panel (b) shows the user on a downhill ramp when the prototype is in the locking position. The first trial demonstrated that the system self-locked while the user was on a ramp without any power input.

The second trial consisted of introducing power through the external pushrim in order to test the motion of the prototype. By moving the external pushrim of the prototype, the power input was transferred from the input arm and thus moving gears 4 and 4′, provoking the motion of gear 1 (output of self-locking PGT) and consequently moving the wheelchair. The subject was told to move the pushrim at the speed he considered appropriate. While pushing the wheelchair through various cycles and then halting the motion, the subject felt comfortable throughout the trial and did not feel at risk of rolling backwards or forwards. Further, the user did not feel the effects of inertia when changing between a stationary position and motion. In Fig. 12 the user is introducing power to the system through the new external rim in both ascending (panel c) and descending (panel d) ramps. The ramp used was 10 % slope. Different repetitions ascending and descending the ramp were carried out.

It is evident that, on one hand, the system self-locks when the power is introduced through the wheel in both ascending and descending trials (Fig. 12, panels a and b). This behaviour prevents the user from going backwards ascending or going downhill while descending. On the other hand the system moves while the power is introduced through the external rim (Fig. 12, panels c and d).

6 Conclusions

In this work, we have described the design of a new propulsion system applied to manual wheelchairs for the ascent or descent of long ramps. The system consists of a self-locking planetary transmission and a push rim through which power is input to the mechanism. With this configuration, it is possible to design a system that makes it easier for the user to ascend long ramps and that self-locks when the user stops inputting power through the push rim. The chair therefore stops without any need for an external braking mechanism to be activated. Although the system is designed especially for climbing long ramps since this is the least favorable situation, it also allows the descent of ramps. In addition, it can be adapted to each user's physical conditions by selecting each transmission ratio according to that user's needs depending on the power that they can transmit.

It has to be emphasized that the system is made up of mechanical components and requires no external elements for its activation or deactivation. This allows the user to push the chair without fearing when it might be descending. Additionally, when they wish to resume motion, they will not need to overcome the force of inertia, but rather simply start pushing the chair again. All this makes the design characteristics of the propulsion system proposed in this work adaptable to any user.

Finally, the transmission was also built and tested on a manual wheelchair. In a qualitative way it has been demonstrated that the system self-locks while both ascending and descending a ramp when the power is introduced through the wheels. It has also been demonstrated that the propulsion system moves the wheelchair when the power is introduced through the external rim. For future works, lighter materials and considerations regarding the size of the device will be taken into account. The device will also be tested on im-

paired users with lower limb injuries and further studies like energy consumption and muscle behaviour will be analysed.

Data availability. All the data used in this article can be obtained upon request from the corresponding author.

Competing interests. The authors declare that they have no conflict of interest.

Edited by: Chin-Hsing Kuo
Reviewed by: two anonymous referees

References

American Gear Manufacturers Association: American National standard?: design manual for enclosed epicyclic metric module gear drivers, American Gear Manufacturers Association, USA, 1988.

Anderson, N. E. and Loewenthal, S. H.: Spur-gear-system efficiency at part and full load, NASA Tech. Rep., 79–46, 1980.

Arnet, U., Van Drongelen, S., Veeger, D. J., and Van Der Woude, L. H. V.: Force application during handcycling and handrim wheelchair propulsion: An initial comparison, J. Appl. Biomech., 29, 687–695, https://doi.org/10.1123/jab.29.6.687, 2013.

Boninger, M. L., Cooper, R. A., Robertson, R. N., and Shimada, S. D.: Three-dimensional pushrim forces during two speeds of wheelchair propulsion, Am. J. Phys. Med. Rehab., 76, 420–426, 1997.

Boninger, M. L., Souza, A. L., Cooper, R. A., Fitzgerald, S. G., Koontz, A. M., and Fay, B. T.: Propulsion patterns and pushrim biomechanics in manual wheelchair propulsion, Arch. Phys. Med. Rehab., 83, 718–723, https://doi.org/10.1053/apmr.2002.32455, 2002.

Choi, Y. O., Lee, H. Y., Lee, M. H., and Kwon, O. H.: Effects of ramp slope on physiological characteristic and performance time of healthy adults propelling and pushing wheelchairs, J. Phys. Ther. Sci., 27, 7–9, https://doi.org/10.1589/jpts.27.7, 2015.

Chow, J. W., Millikan, T. A., Carlton, L. G., Chae, W. S., Lim, Y. T., and Morse, M. I.: Kinematic and Electromyographic Analysis of Wheelchair Propulsion on Ramps of Different Slopes for Young Men With Paraplegia, Arch. Phys. Med. Rehab., 90, 271–278, https://doi.org/10.1016/j.apmr.2008.07.019, 2009.

Dallmeijer, A. J., Kappe, Y. J., Veeger, D. H. E. J., Janssen, T. W. J., and van der Woude, L. H. V.: Anaerobic power output and propulsion technique in spinal cord injured subjects during wheelchair ergometry, J. Rehabil. Res. Dev., 31, 120–128, 1994.

De Groot, S., Veeger, H. E. J., Hollander, A. P., and Van der Woude, L. H. V.: Consequence of feedback-based learning of an effective hand rim wheelchair force production on mechanical efficiency, Clin. Biomech., 17, 219–226, https://doi.org/10.1016/S0268-0033(02)00005-0, 2002.

de Groot, S., Zuidgeest, M., and van der Woude, L. H. V.: Standardization of measuring power output during wheelchair propulsion on a treadmill. Pitfalls in a multi-center study, Med. Eng. Phys., 28, 604–612, https://doi.org/10.1016/j.medengphy.2005.09.004, 2006.

Del Castillo, J. M.: The analytical expression of the efficiency of planetary gear trains, Mech. Mach. Theory, 37, 197–214, https://doi.org/10.1016/S0094-114X(01)00077-5, 2002.

Diab, Y., Ville, F., and Velex, P.: Prediction of Power Losses Due to Tooth Friction in Gears, Tribol. T., 49, 266–276, https://doi.org/10.1080/05698190600614874, 2006.

Flemmer, C. L. and Flemmer, R. C.: A review of manual wheelchairs Claire, Disabil. Rehabil. Assist. Technol., 11, 177–187, https://doi.org/10.3109/17483107.2015.1099747, 2016.

Howarth, S. J., Pronovost, L. M., Polgar, J. M., Dickerson, C. R., and Callaghan, J. P.: Use of a geared wheelchair wheel to reduce propulsive muscular demand during ramp ascent: Analysis of muscle activation and kinematics, Clin. Biomech., 25, 21–28, https://doi.org/10.1016/j.clinbiomech.2009.10.004, 2010.

Hwang, S. C., Lee, J. H., Lee, D. H., Han, S. H., and Lee, K. H.: Contact stress analysis for a pair of mating gears, Math. Comput. Model., 57, 40–49, https://doi.org/10.1016/j.mcm.2011.06.055, 2013.

Koontz, A. M., Cooper, R. A., Boninger, M. L., Yang, Y., Impink, B. G., and van der Woude, L. H. V.: A kinetic analysis of manual wheelchair propulsion during start-up on select indoor and outdoor surfaces, J. Rehabil. Res. Dev., 42, 447, https://doi.org/10.1682/JRRD.2004.08.0106, 2005.

Kwarciak, A. M., Yarossi, M., Ramanujam, A., Dyson-Hudson, T. A., and Sisto, S. A.: Evaluation of wheelchair tire rolling resistance using dynamometer-based coast-down tests, J. Rehabil. Res. Dev., 46, 931–938, https://doi.org/10.1682/JRRD.2008.10.0137, 2009.

Li, S.: Contact Stress and Root Stress Analyses of Thin-Rimmed Spur Gears With Inclined Webs, J. Mech. Design, 134, 51001, https://doi.org/10.1115/1.4006324, 2012.

Lin, C.-J., Lin, P.-C., Su, F.-C., and An, K.-N.: Biomechanics of wheelchair propulsion, J. Mech. Med. Biol., 9, 229–242, https://doi.org/10.1142/S0219519409002948, 2009.

Meginniss, S. M. and SanFrancisco, A. S.: Two-Speed manual wheelchair wheel, United States Pat. Appl. Publ., 53, US 2006/0197302 A1, 2006.

Moreira, P., Ramôa, P., and Flores, P.: Design of a new knee orthosis locking system, Proceedings of the ASME 2013 International Mechanical Engineering Congress and Exposition IMECE2013, 15–21 November 2013, San Diego, California, USA, https://doi.org/10.1115/IMECE2013-64276, 2016.

Müller, H.: Epicyclic drive trains: Analysis, synthesis, and applications, Wayne University Press, Detroit, USA, 1982.

Patil, S., Karuppanan, S., Atanasovska, I., and Wahab, A. A.: Frictional Tooth Contact Analysis along Line of Action of a Spur Gear Using Finite Element Method, Proc. Mat. Sci., 5, 1801–1809, https://doi.org/10.1016/j.mspro.2014.07.399, 2014.

Richter, W. M., Rodriguez, R., Woods, K. R., and Axelson, P. W.: Stroke Pattern and Handrim Biomechanics for Level and Uphill Wheelchair Propulsion at Self-Selected Speeds, Arch. Phys. Med. Rehab., 88, 81–87, https://doi.org/10.1016/j.apmr.2006.09.017, 2007.

Robertson, R. N., Boninger, M. L., Cooper, R. A., and Shimada, S. D.: Pushrim forces and joint kinetics during wheelchair propulsion, Arch. Phys. Med. Rehab., 77, 856–864, https://doi.org/10.1016/S0003-9993(96)90270-1, 1996.

Salgado, D. R. and Castillo, J. M.: Conditions for self-locking in planetary gear trains, J. Mech. Des.-T. ASME, 129, 960–968, https://doi.org/10.1115/1.2748449, 2007.

Sonenblum, S. E., Sprigle, S., and Lopez, R. A.: Manual Wheelchair Use: Bouts of Mobility in Everyday Life, Rehabil. Res. Pract., 2012, 1–7, https://doi.org/10.1155/2012/753165, 2012.

Sprigle, S. and Huang, M.: Impact of Mass and Weight Distribution on Manual Wheelchair Propulsion Torque, Assist. Technol., 27, 226–235, https://doi.org/10.1080/10400435.2015.1039149, 2015.

van der Woude, L., Dallmeijer, A., Janssen, T., and Dirjkan, V.: Alternative Modes of Manual Wheelchair Ambulation, Am. J. Phys. Med. Rehab., 80, 765–777, doi:10.0894-9115/01/8010-0765/0, 2001.

van der Woude, L. H., Hendrich, K. M., Veeger, H. E. J., van Ingen Schenau, G. J., Rozendal, R. H., de Groot, G., and Hollander, A. P.: Manual wheelchair propulsion: effects of power output on physiology and technique, Med. Sci. Sport. Exer., 20, 70–78, https://doi.org/10.1249/00005768-198802000-00011, 1988.

Van Der Woude, L. H. V., Geurts, C., Winkelman, H., and Veeger, H. E. J.: Measurement of wheelchair rolling resistance with a handle bar push technique, J. Med. Eng. Technol., 27, 249–258, https://doi.org/10.1080/0309190031000096630, 2003.

van der Woude, L. H. V., de Groot, S., and Janssen, T. W. J.: Manual wheelchairs: Research and innovation in rehabilitation, sports, daily life and health, Med. Eng. Phys., 28, 905–915, https://doi.org/10.1016/j.medengphy.2005.12.001, 2006.

Vanlandewijck, Y., Theisen, D., and Daly, D.: Wheelchair propulsion biomechanics: implications for wheelchair sports, Sport. Med., 31, 339–367, https://doi.org/10.2165/00007256-200131050-00005, 2001.

Veeger, H. E. J., Van Der Woude, L. H. V., and Rozendal, R. H.: Load on the Upper Extremity in Manual Wheelchair Propulsion, J. Electromyogr. Kines., I, 270–280, https://doi.org/10.1016/1050-6411(91)90014-V, 1991.

Xu, H. and Kahraman, A.: A Frictional Efficiency Loss Model for Helical Gears, ASME 2005 Int. Des. Eng. Tech. Conf. Comput. Inf. Eng. Conf., 1–12, https://doi.org/10.1115/DETC2005-85243, 2005.